PNNL-13341

Testing and Analysis of Consolidated Sludge Samples from the 105 K East Basin Floor and Canisters

P. R. Bredt
C. H. Delegard
A. J. Schmidt
K. L. Silvers

December 1999

Prepared for
Fluor Hanford

Work supported by
the U.S. Department of Energy
under Contract DE-AC06-76RLO 1830

Pacific Northwest National Laboratory
Richland, Washington 99352

DISCLAIMER

PACIFIC NORTHWEST NATIONAL LABORATORY
operated by
BATTELLE
for the
UNITED STATES DEPARTMENT OF ENERGY
under Contract DE-AC06-76RL01830

Printed in the United States of America

Available to DOE and DOE contractors from the
Office of Scientific and Technical Information,
P.O. Box 62, Oak Ridge, TN 37831-0062;
ph: (865) 576-8401
fax: (865) 576-5728
email: reports@adonis.osti.gov

Available to the public from the National Technical Information Service,
U.S. Department of Commerce, 5285 Port Royal Rd., Springfield, VA 22161
ph: (800) 553-6847
fax: (703) 605-6900
email: orders@ntis.fedworld.gov
online ordering: http://www.ntis.gov/ordering.htm

This document was printed on recycled paper.
(8/00)

Abstract

The testing reported here was performed on K East Basin consolidated sludge samples to generate data needed for the evaluation and design of the systems that will be used to disposition the K Basin sludge to T-Plant for interim storage. The tests were conducted by Pacific Northwest National Laboratory from May through November 1999 under the direction of the Spent Nuclear Fuel (SNF) Project. The samples used in the work discussed here were collected by the SNF Characterization Project from the KE Basin floor and canisters during March and April 1999. These samples (3 from the floor and 3 from the canisters) were shipped to the storage pool at the Postirradiation Testing Laboratory (327 Building) and later transferred to the PNNL Radiochemical Processing Laboratory (325 Building), where they were recovered for testing and analysis.

Testing activities presented in this report include particle size measurement via wet sieving, sludge settling and sludge density measurements, sludge shear strength measurement, and measurement of sludge dissolution enthalpy to ascertain the uranium metal content of the sludge. Section 1.0 provides the summary and conclusions to date. Section 2.0 describes the consolidated sample container system, the sample collection and transfer, inspection, and recovery of the samples for testing. Section 3.0 describes the testing methodologies and presents the results and analyses.

Contents

Figures

Figures (continued)

Tables

1.0 Summary and Conclusions

This report describes testing performed on KE Basin consolidated sludge samples to generate data needed for the evaluation and design of the systems that will be used to disposition the K Basin sludge to T-Plant for interim storage. The Pacific Northwest National Laboratory (PNNL) conducted the work in May through November 1999 under the direction of the Spent Nuclear Fuel (SNF) Sludge Project. The SNF Characterization Project collected six samples for these analyses and tests from the KE Basin floor (3 samples) and fuel canisters (3 samples) in March through April 1999 using a consolidated sampling technique. These samples were then shipped to the storage pool at the Postirradiation Testing Laboratory (327 Building) and later transferred to and recovered at PNNL's Radiochemical Processing Laboratory (325 Building).

After sample recovery, a series of tests were conducted to provide time-sensitive data required to understand the characteristics of the consolidated sludge samples that are important to developing the systems for shipping and storing the K Basin sludge in T-Plant. Because the uranium metal component (and other reactive components) in the sludge samples undergoes oxidation reactions, the composition of the sludge changes with time. In the radiological shielded processing cells within the 325 Building, the sludge samples are stored at about 30°C, while the sludge in the K Basin pools is maintained at about 10°C. This temperature differential, as well as sludge handling, can result in degradation of the samples over time. This aging can affect many of the properties of the sludge. As a result, for the testing initiated in FY 1999, efforts were focused on the most important time-dependent testing. These testing activities include particle size measurement via wet sieving; sludge settling and sludge density measurements; sludge shear strength measurement; and the measurement of sludge dissolution enthalpy to ascertain the uranium metal content of the sludge. The tests were performed in accordance with the direction provided in the Sample and Analysis Plan for the consolidated sludge samples (Baker et al. 1999). The results of these tests are summarized below.

Consolidated Sludge Sample Receiving and Recovery

Sludge containers were transferred to the 325 Building's High Level Radiochemistry Facility (325A HLRF) between May 7 and May 13, and were inspected for indications of excessive gas generation during shipping. No evidence for excessive gas generation was observed. Samples were then recovered from the large consolidated sample containers (10.3 L) into smaller, more convenient containers. To provide the necessary quantities of sludge for the testing activities, two consolidated sludge samples, collected from the KE fuel canisters, were combined into a composite sample (consolidated canister sludge composite).

Wet Sieving

Sieving is a technique that uses meshes or perforated membranes to separate particles within a material into unique particle size fractions. In wet sieving, an aqueous fluid is introduced on top of the material. The fluid aids in the transport of the particles from one mesh to the next, as well as preventing the particles from drying out. For the consolidated sludge samples, two sieving campaigns were conducted: small-scale sieving to characterize the particle size distribution, and large-scale sieving to generate sufficient quantities of test material. In addition, dry particle density measurements were made on some of the particles from the discrete fractions of the sieved sludge.

Green and yellow particles were observed in all of the samples. During work on samples collected from previous KE Basin characterization campaigns, these colors were associated with samples containing high levels of uranium oxide. Sieving of one of the consolidated floor sludge samples (KC-5) revealed organic ion exchange resin beads on several of the sieves. Since sample KC-5 was collected from locations in the basin that were away from both highly corroded fuel and away from organic ion exchange beads, the presence of organic ion exchange resin beads was not anticipated.

The dry particle density measurements showed that, for the canister composite sludge, particle density distinctly increases with decreasing particles size (i.e., the smaller particles are more dense). The finding that dry particle density changes with particle size is very significant. In a previous report on the particle size distribution of the various K Basin sludge types (Bredt et al. 1999), it was assumed that the sludge density was uniform across all particle size ranges.

Results from the wet sieving and particle density measurements were compared and integrated with previous particle size distribution data. In the previous analysis (Bredt et al. 1999), sludge from the KE fuel canisters was found to be relatively coarse material with roughly 50 wt% below 710 μm. However, the consolidated canister sludge composite was much finer, with approximately 90 wt% below 500 μm. While one of the consolidated floor sludge samples closely agreed with the previous floor sludge data (~92 wt%, below 500 μm), sample KC-5 is much coarser, with only 46 wt% below 500 μm. In summary, integrating the new data with the earlier data leads to revised particle size distribution curves, in which the floor sludge appeared coarser and the canister sludge appeared finer than previously projected.

Results from the analysis of the sieving data are being incorporated into a revision of the K Basin Materials Design Basis Feed Document (Pearce et al. 1998).

Settling Rates and Settled Sludge Density Measurements

The consolidated sludge samples were place in graduated cylinders, mixed with K Basin water, and allowed to settle. The settling rates and the densities of the settled sludge were measured. The settled sludge density measurements will be used to refine KE Basin sludge inventory projections. Settling rate information provides insight into what can be expected in the K Basin pool, in terms of water clarity, when fuel canisters and sludge are moved.

The settling rate and settled sludge density data from the consolidated sludge samples agree reasonably well with previous data from KE floor sludge samples (Makenas et al. 1996) and KE canister sludge samples (Makenas et al. 1997).

For sample KC-2/3, the settled sludge density of particles greater than 250 μm was essentially identical to the settled sludge density of the particles less than 250 μm. This finding was unexpected, as dry particle density was shown to change significantly with particle size.

Shear Strength Measurements

The sludge shear strength was measured to provide information on how much shear will be required to mobilize the sludge for transport and to understand how the sludge sample will retain and release gas bubbles. Reactive components in the sludge (e.g., uranium metal) generate gas, which is primarily made

up of hydrogen. Radiolysis of water will also generate some hydrogen gas. Depending upon the shear strength of the sludge, the gas bubbles will either quickly pass through the sludge and be released, or the gas bubbles will be retained in the sludge and be released episodically. An additional possibility is that spanning gas bubbles can form and push the sludge up the storage vessel as a plug. The gas retention and gas release behavior of the sludge will affect the design of the systems used to transport and store the sludge in T-Plant.

Results from the shear strength measurements suggest that K Basin sludges can form spanning bubbles during storage unless steps are taken to mitigate this hazard. The shear strength measurement can also be used to develop surrogates for testing bubble mitigation design features.

Dissolution Enthalpy Measurements

Fractions of sludge samples containing particles greater than 250 μm (designated as P250) were placed in a calibrated calorimeter and dissolved in nitric acid. The enthalpy of the dissolution was determined and compared with known enthalpies of dissolution of uranium metal and UO_2 in nitric acid. The measured enthalpies of the samples were compared with the known enthalpies and used to estimate uranium metal content of the sludge samples. The uranium metal content and the particle size distribution of the uranium metal largely determine amount and rates of gas and heat generation within the sludge. In turn, the heat and gas generation rates affect the design and cost of the sludge transportation and storage systems.

The measured enthalpies of reaction strongly suggest the presence of uranium metal in the P250 canister composite sludge (4 to 9 wt% uranium metal, settled sludge basis). The data do not provide evidence of uranium metal in one of the floor samples, which was collected between fuel canister samples. However, for the other floor sample evaluated (KC-5 P250), collected away from the fuel canisters, the data suggest some uranium may be present (0.7 wt% uranium metal, settled sludge basis). In estimating the quantity of uranium metal present, it was assumed that the sludge samples were made up entirely of uranium metal and UO_2. For the KE canister sludge, this is a reasonable assumption, as previous data have shown the sludge to be 80 to 90 wt% uranium (dry weight basis) (Makenas et al. 1997). However, previous data show that the floor sludge is only 3 to 33 wt% uranium (Makenas et al. 1996). If it was assumed that 70% of the floor sludge was inert in nitric acid (e.g., SiO_2), then the projected uranium metal content of the KC-5 P250 sample would be 2.3%.

2.0 Sampling Receipt, Inspection, and Recovery

This section describes the consolidated sample container system used for obtaining and shipping sludge samples, inspections conducted when the samples were received at 325 Building, and activities conducted to recover samples from the containers. The sample containers were inspected to assess the condition of the samples and any gas generation during transport. Gas generation within the sample container from the reaction of uranium metal with water was anticipated. Previous observations with similar sludge material indicated that agitation of the sludge during handling and shipping can result in hydrogen gas generation.

2.1 Sample Collection and Transfer

The samples used for the testing discussed here were collected from the KE Basin floor and fuel canisters by the SNF Characterization Project (Table 1). The samples were collected during March and April 1999 using the Consolidated Sludge Sampling System described in Hecht (1999). Consolidated sample KC-1 was collected using the consolidated sludge sampling system in the "single pull" mode. A vacuum was applied to the head of a 10.3-L stainless steel container, drawing sludge into the container until it was full enough to activate a check valve and stop the sampling process. In the consolidated sampling mode used to collect the remaining samples (KC-2 through KC-6), a 5-μm stainless steel filter replaced the check valve, with the same vacuum technique employed to draw sludge and basin water into a 10.3-L container. In this mode, the filter causes sludge to be trapped in the canister while the excess water is returned to the basin. Consequently, much larger amounts of sludge from several different sampling locations can be consolidated within one 10.3-L container. This system is an economical method for providing large representative sludge samples (Petersen 1999). Pitner (1999) provides a detailed discussion of the sampling process and general observations made during sludge sample collection operations.

After collection, the consolidated samples were stored in the 327 Building storage pool and shipped to the 325A HLRF between May 7 and 13, 1999. Table 2 provides information listed in the chain-of-custody that accompanied the samples to the 325 Building, along with other sampling information and the estimated mass of sludge recovered from each container. Some K Basin water also remained in the container, even with the filter in place. Work conducted on these samples is documented in test instructions and Battelle Northwest Laboratory Record Book 56479.

Table 1. Sampling Location and Material Information for Consolidated Samples Used in This Study

Container	Material Type	Sampling Locations	Fuel Canister Type	Barrel Material
KC-1[a]	Canister Sludge From Highly Damaged Fuel	4569E	Mark 0	Aluminum
KC-2	Canister Sludge From Highly Damaged Fuel	668E & W 2229E 4571E 6071W	Mark 0 Mark 0 Modified Co-Product Mark 0	Aluminum
KC-3	Canister Sludge From Moderately Damaged Fuel	4850W 4869E 3125W 2905E 450E 455W	Mark 0 Mark 0 Mark 0 Mark 0 Mark 0 Mark 0	Aluminum
KC-4[b]	Floor Sludge From Between Slotted Canister Barrels Containing Highly Damaged Fuel	0549 4573 5465	Modified Co-Product Modified Co-Product Modified Co-Product	Aluminum
KC-5[c]	Floor Sludge From Areas of Deep Sludge Typically Away from Highly Corroded Fuel and Areas with High Concentrations of IXM Beads	4648 3133 0548	Mark II Mark 0 Modified Co-Product	Stainless Steel Aluminum Aluminum
KC-6[c]	Floor Sludge Containing High Concentrations of IXM Beads	6758	Mark 0	Aluminum

[a] Sample KC-1 was collected with the consolidated sampling system operated in the "single-pull" mode.
[b] Sample KC-4 was collected from the floor of the basin; however, the sampling locations were near Modified Co-Product barrels.
[c] Samples KC-5 and KC-6 were collected from the basin floor, but barrels were previously in these locations.

Table 2. Chain-of-Custody Information for Samples Shipped from 327 Building to 325A HLRF. The estimated amount of sludge recovered from the container is also listed.

Container	Sampling Locations	Collection Date	Collection Time	Container Serial Number	Estimated[a] Sludge	Check Valve (CV) or Filter (F)
KC-1	4569E	4/12/99	11:47	99-01-A-V (Lid) 99-01-B-V (Body)	250 ml	CV
KC-2	668E & W 2229E 4571E 6071W	3/4/99 3/8/99 3/9/99 3/13/99	14:20 14:40 13:28 09:54	99-03-A-F (Lid) 99-03-B-F (Body)	2,200 g	F
KC-3	4850W 4869E 3125W 2905E 450E 455W	4/1/99 4/6/99 4/7/99 4/7/99 4/8/99 4/8/99	13:40 10:01 13:50 15:08 13:08 13:55	99-08-A-F (Lid) 99-08-B-F (Body)	~1 L 950 g	F
KC-4	0549 4573 5465	3/30/99 3/31/99 3/31/99	14:27 10:59 14:17	99-04-A-F (Lid) 99-04-B-F (Body)	2 to 3 L, 2,600 g	F
KC-5	4648 3133 0548	3/29/99 3/29/99 3/30/99	11:04 13:42 10:04	99-05-A-F (Lid) 99-05-B-F (Body)	1,300 g	F
KC-6	6758 6758	3/13/99 3/26/99	15:39 10:09	99-07-A-F (Lid) 99-07-B-F (Body)	6 L 7,400 g	F

[a] Estimated mass and/or volume of sludge recovered from the shipping containers. Mass and volume data were not collected in all cases. These data should not be used to estimate sludge densities. Because of the relatively large sample and container masses, a limited precision scale (±100 g) was used (in accordance with the approved test plan). Therefore, the mass values in this table are for indication only.

2.2 Consolidated Sample Container Inspection

Within 4 hours of receipt at 325A, the 10.3-L containers were vented by rotating the brass stem valve three complete turns. The technicians noted that, upon venting, water leaked out of the vent stems on three of the containers: KC-2, KC-3, and KC-4. The volume of water released was estimated to be approximately 2 ml, 3 ml, and 10 ml, respectively. The containers had been sealed under approximately 20 ft of water in the 327 Building pool basin, while the 325 Building hot cells were at ambient pressure, which could explain this small amount of pressurization. Therefore, no strong indications of gas generation were evident in any of the consolidated sludge samples during transport between the 327 and 325 buildings.

A fixed-volume (~400 ml) stainless steel headspace vessel was attached to the top of each 10.3-L consolidated sample container to mitigate a pressurization and/or flammable gas hazard. These fixed-

volume vessels were purged with an inert gas before being attached. The goal of these headspace vessels was to prevent overpressurization by providing volume for gas generated during shipment. Purging the headspace vessels with inert gas also reduced the potential flammability hazard.

Following the venting described above, the headspace vessels were removed from the containers and weighed. These weights are listed in Table 3. All of the headspace vessels had approximately the same weight, with the exception of KC-1. Therefore, it was assumed that only the KC-1 headspace vessel contained any sample material. Subtracting the mass of the KC-1 headspace vessel from the average mass of the remaining five vessels suggests the KC-1 headspace vessel retained ~290 g of material. The KC-1 headspace vessel was drained and found to contain basin water. In the single pull mode used for sample KC-1, the sampling container utilizes a float valve that prevents water from exiting the container while it is in an upright position. During shipping, this container was laid on its side, and the float valve likely opened, allowing water to enter the headspace vessel.

Table 3. Weight of Headspace Vessels Following Venting of Sample Containers

Consolidated Sample Container ID	Headspace Vessel ID	Headspace Vessel Mass, g
KC-1	1	1254.67
KC-2	2	958.09
KC-3	3	968.13
KC-4	4	960.17
KC-5	5	966.25
KC-6	6	965.82
Average (KC-2 through KC-6)		963.69

2.3 Recovery of Sludge from Consolidated Sample Containers

Sludge was recovered from the sample containers between May 26 and June 5, 1999. The sludge was vacuum transferred out of the containers using a probe made of 3/8-in. stainless steel tubing connected to a collection vessel by nylon-reinforced silicone tubing. Collection vessels included 500-ml glass jars, 2-L glass graduated cylinders, and 10-L glass carboys, depending on the volume of sludge anticipated.

A 10-L glass carboy was used during the first step of the recovery. Vacuum was applied to the vacuum train, and the probe was then slowly lowered into the sample container. The first material through the train was clear K Basin water. The clarity of water transferred to the collection vessel was monitored. For sample KC-6, all material in the shipping canister was transferred to the 10-L glass carboy. For the other samples, as soon as the water clarity dropped, indicating the probe was nearing the settled solids layer, the carboy was removed and a smaller collection vessel was used to collect the solids. The solids recovered from sample KC-1 were transferred to a 1-L glass jar. For samples KC-2 through KC-5, solids were transferred to 6-L stainless steel pressure cookers. Pressure cookers were chosen for several reasons: 1) given the sample size, a large metal container provided safer storage than a large glass vessel; 2) the seal on the pressure cooker was sufficient to prevent evaporation; and 3) the pressure cooker seal provided a passive mechanism to prevent overpressurization that could result from anticipated hydrogen generation.

Following recovery, samples were monitored (and continue to be monitored) on a regular basis, approximately weekly, to assure standing liquid remained on the solids. During previous K Basin

sampling campaigns, it was observed that most samples vessels did not seal and tended to dry over a period of weeks to months. Although several different rewetting techniques were attempted on completely dry samples (no visible liquid), complete drying tended to irreversibly alter the physical properties of the sludge. In most cases, the completely dried sludge formed hard chunks that could only be reconstituted by stirring and sonication (40 Watts for several minutes). However, even after very aggressive rewetting efforts, the behavior of the reconstituted sludge was altered relative to the fresh sludge.

For the testing with the consolidated sludge samples described here, standing liquid is removed from the mother samples before removing subsamples. This liquid is returned a few minutes later minus some water left in transfer containers and syringes. When needed, additional water from the respective carboys is transferred to the solids to prevent drying. As a result of this subsampling and sample handling protocol, it is not possible to determine the extent of evaporative loss for these samples.

2.4 Recovery of Sludge from Filters

When sample containers KC-2 through KC-6 were opened, the 5-μm stainless steel filters were found to be caked with sludge. Attempts to remove the wet sludge using brushes and agitation were unsuccessful, so the filters were allowed to dry at ambient hot cell temperatures (~32°C). Consequently, the residual sludge on the dried filters could be removed using a stainless steel brush. Table 4 lists the mass of sludge recovered from each of the filters. The dried sludge was added to the rest of the wet sludge recovered from the containers. Figures 1 through 5 show the filters before and after cleaning. It is not known how well the clumps of dried sludge fines (Figures 1 through 5) rewetted and de-agglomerated after being added back to the wet sludge. It is possible that some of these clumps retained their size and upwardly skewed the results from the sieving analysis (Section 3.2).

Table 4. Mass of Dry Sludge Recovered from the Stainless Steel Filters

Sample Container	Dry Sludge Mass, g
KC-2	15.31
KC-3	Not Weighed
KC-4	52.21
KC-5	74.77
KC-6	31.20

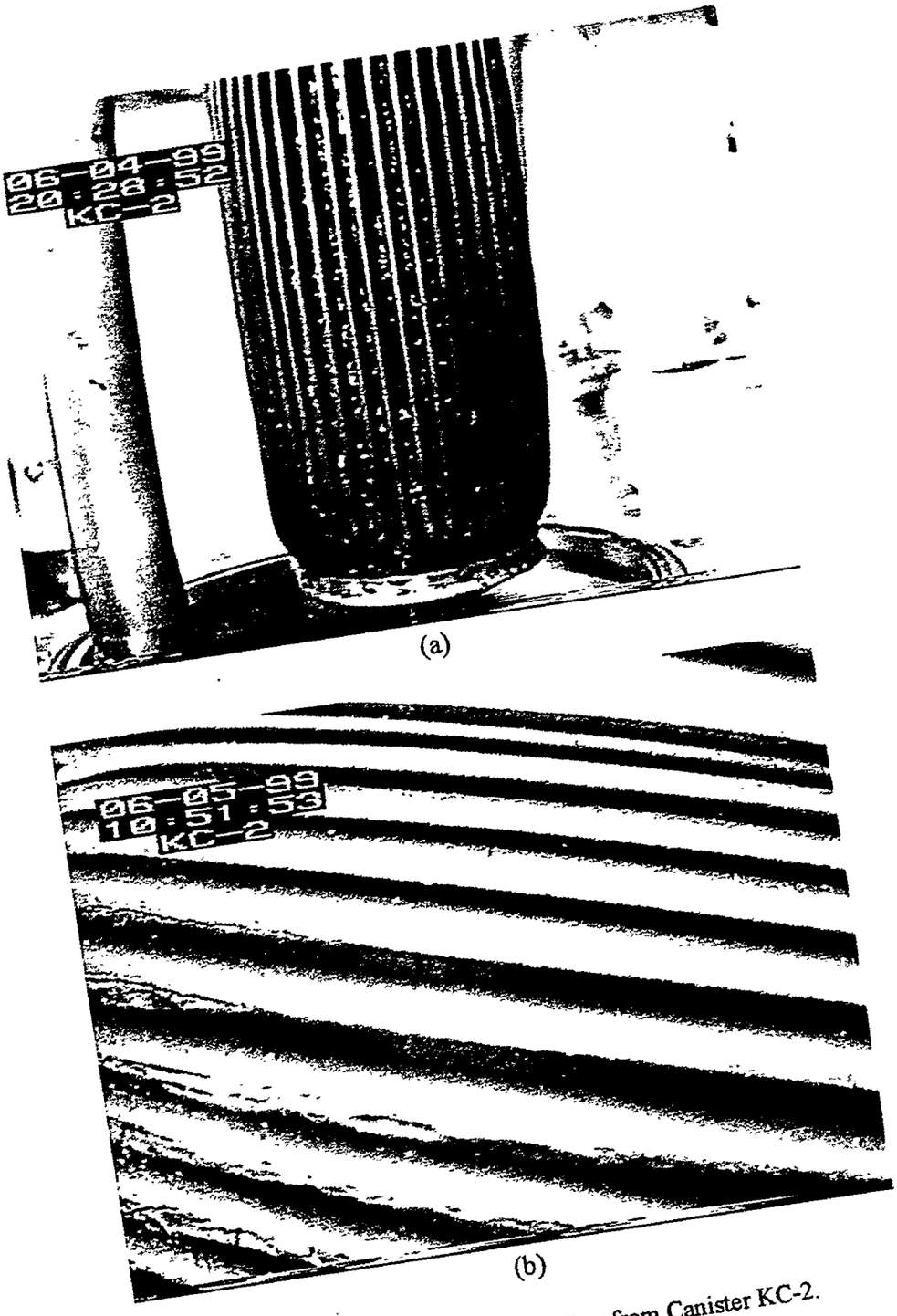

Figure 1. Solids Retained on the Filter from Canister KC-2.
(a) wet solids on the filter, and
(b) air-dried solids on the filter.

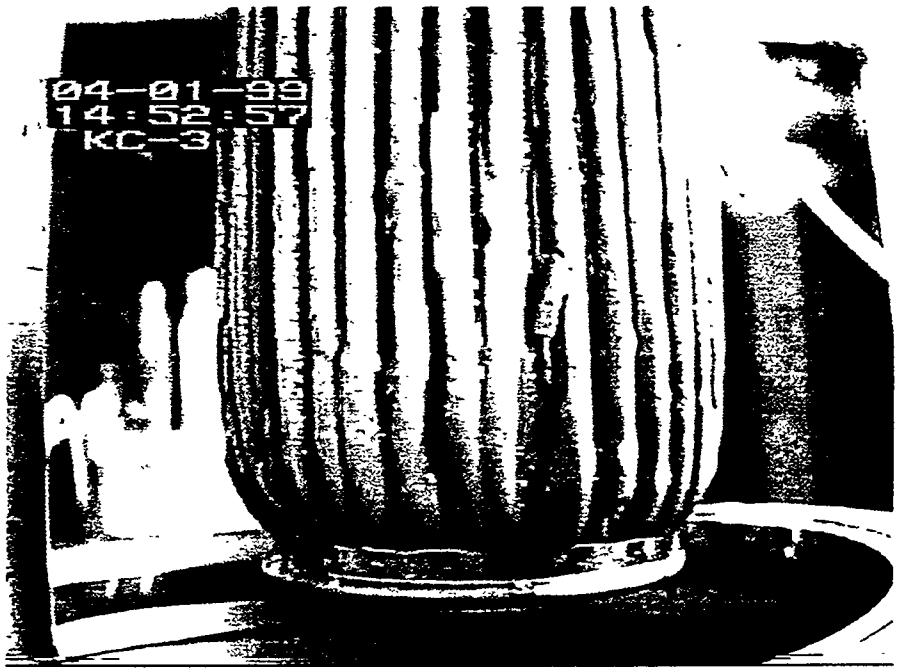

(a)

(b)

Figure 2. Solids Retained on the Filter from Canister KC-3.
(a) wet solids on the filter, and
(b) solids recovered from the air-dried filter using a stainless steel brush.

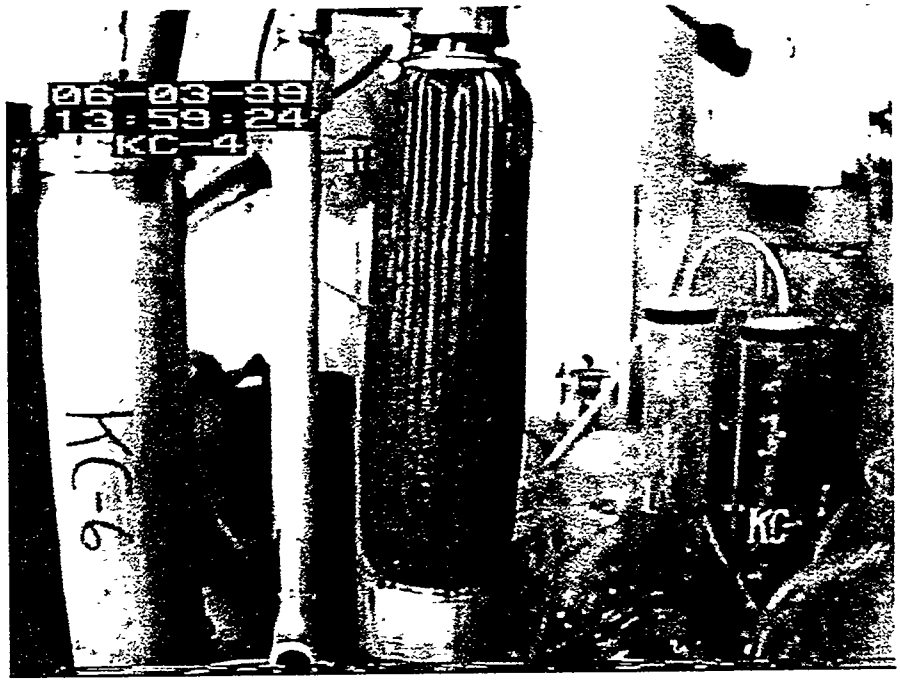

(a)

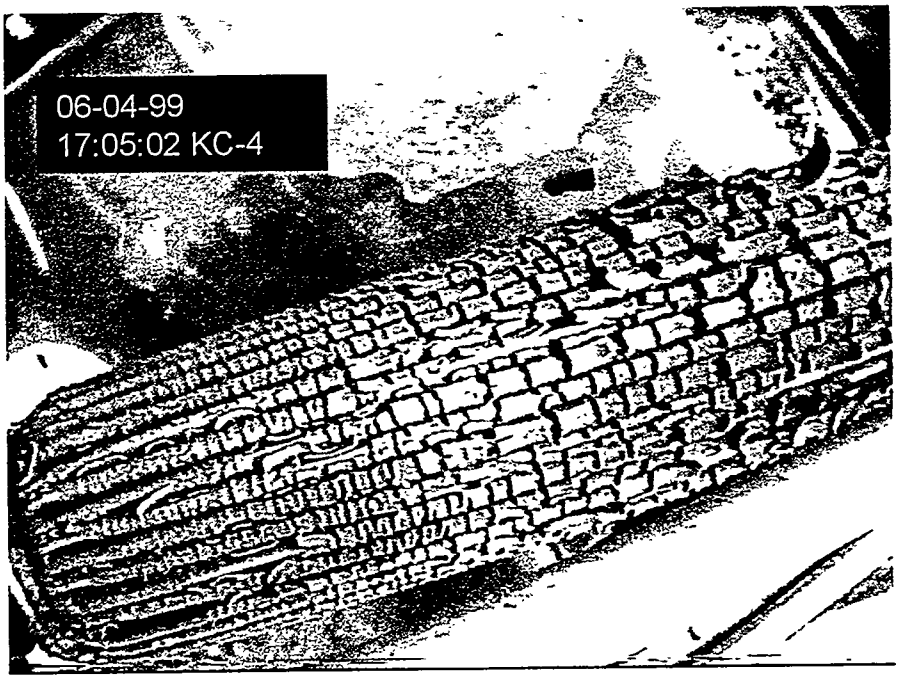

(b)

Figure 3. Solids Retained on the Filter from Canister KC-4.
(a) wet solids on the filter, and
(b) same filter and solids air-dried.

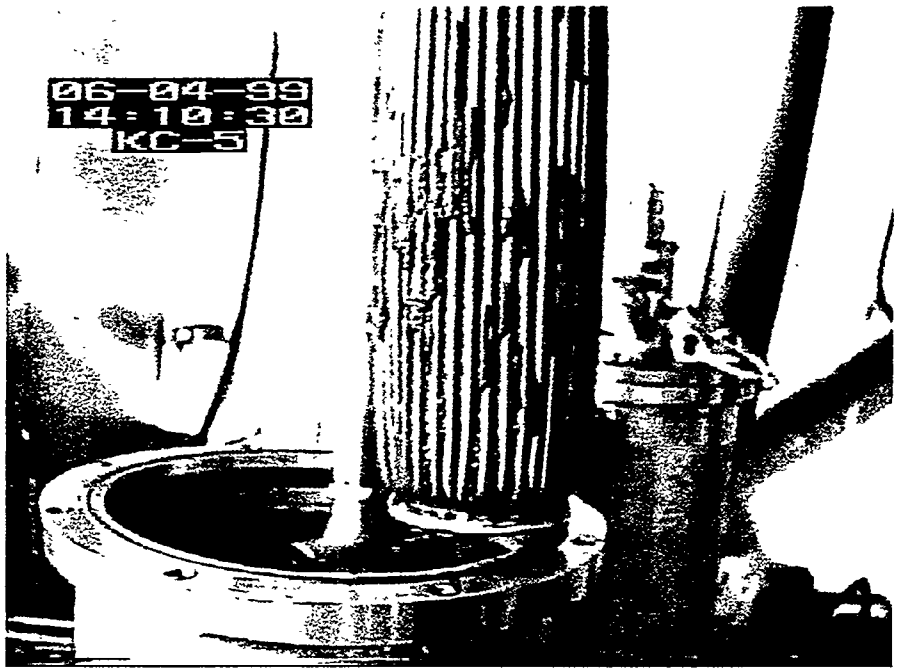

(a)

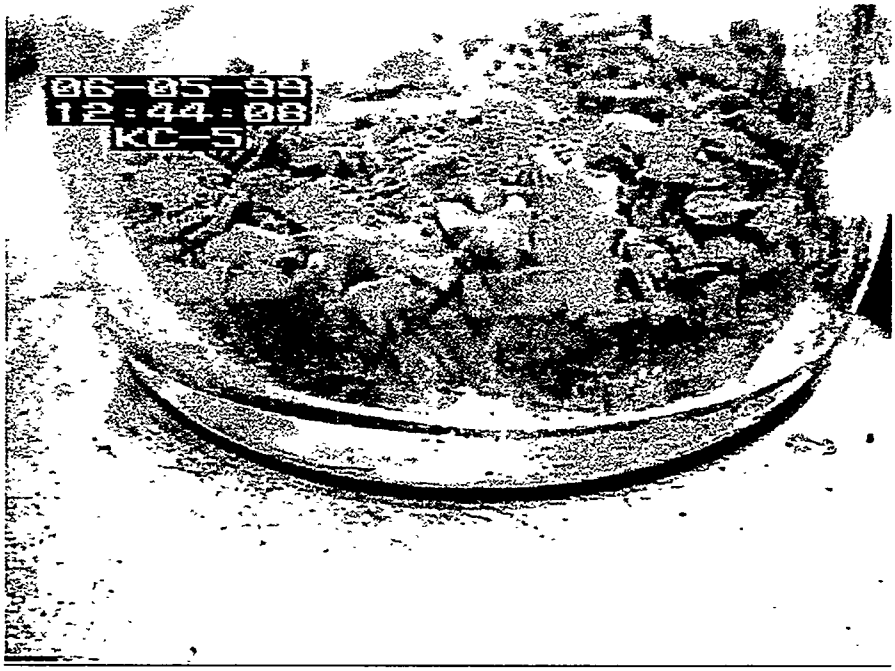

(b)

Figure 4. Solids Retained on the Filter from Canister KC-5.
(a) wet solids on the filter, and
(b) solids recovered from the air-dried filter using a stainless steel brush.

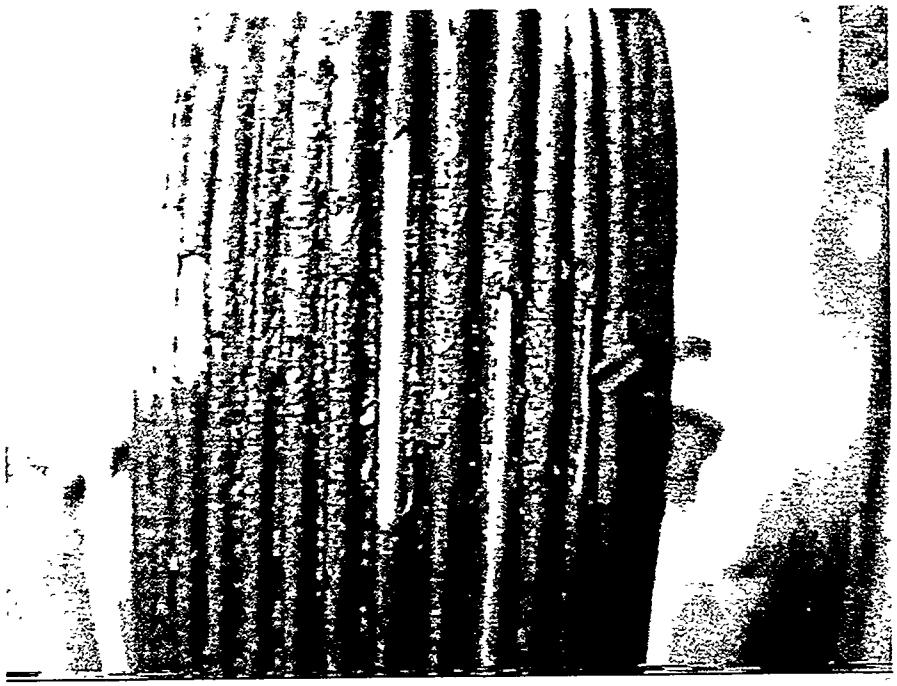

(a)

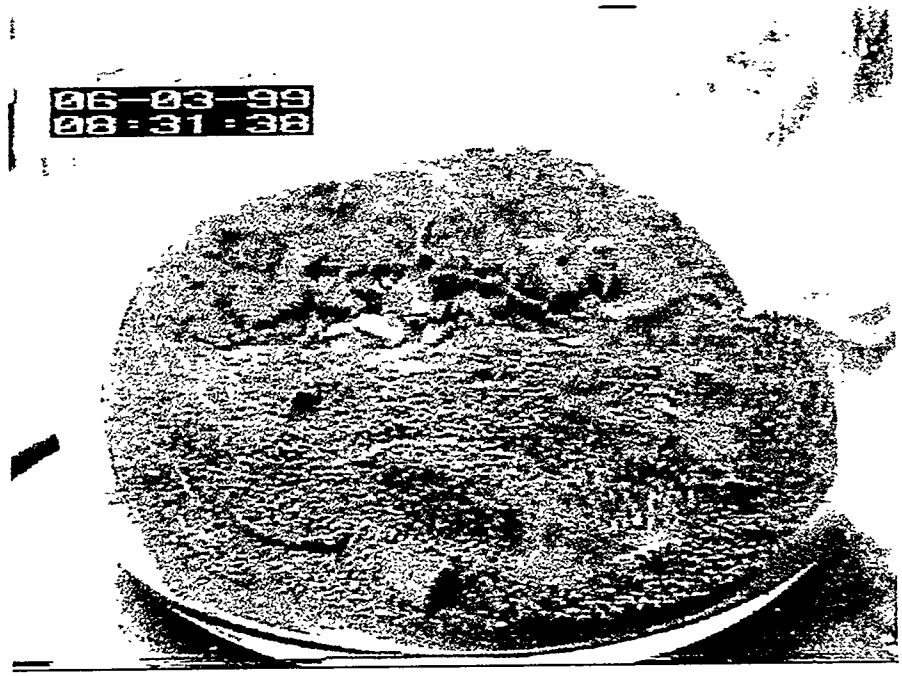

(b)

Figure 5. Solids Retained on the Filter from Canister KC-6.
(a) wet solids on the filter, and
(b) solids recovered from the air-dried filter using a stainless steel brush.

3.0 Test Methods, Analyses, and Results

For the FY 1999 testing, efforts were focused on the most important time-dependent testing. Once collected, sludge samples continue to age with time and change further from the sludge as contained in the K Basin. Testing activities conducted to analyze the consolidated sludge sample characteristics included particle size measurement via wet sieving, sludge settling and sludge density measurements, sludge shear strength measurement, and the measurement of sludge dissolution enthalpy to ascertain the uranium metal content of the sludge.

3.1 Compositing

Early in the testing, it was determined that two of the consolidated sludge samples collected from fuel canisters would need to be combined (composited) to provide the necessary sludge fractions for all planned testing activities. All available materials from samples KC-2 and KC-3 were composited. Sample KC-2 was composed of sludge collected from KE Basin canisters containing highly damaged fuel. Sample KC-3 was composed of sludge collected from KE Basin canisters containing moderately damaged fuel. Sample KC-1, collected from a KE fuel canister using the single pull mode, was left as a unique sample and not added to the composite. Sample KC-1 is a comprehensive sludge sample, with no influence of filtering excess water through a 5-μm filter. It provides a comparison for the KC-2 and KC-3 samples where excess water (and potentially some very fine sludge) was exhausted through the 5-μm filter.

The composite sample is referred to here as the KC-2/3 composite. An limited-precision scale with a unit sensitivity of ~100 g was used in preparing the composite (see footnote on Table 2). Approximately 2100 g of settled sludge from sample KC-2 were added to the composite and approximately 860 g settled sludge from sample KC-3. No attempt was made to determine the water content of the sludges prior to compositing, so the actual ratio of solids in the composite is not known.

3.2 Small-Scale Wet Sieving

Samples of material from Canisters KC-1, KC-3, KC-4, KC-5, and the KC-2/3 composite were sieved to assess the particle size distribution in the sludge. Through the use of meshes or perforated membranes, sieving separates particles within a material into unique particle size fractions. Since K Basin processing operations are planned to be performed on wet material, a wet sieving technique was used. In wet sieving, an aqueous fluid is introduced on top of the material. The fluid aids in the transport of the particles from one mesh to the next, as well as preventing the particles from drying out. After completing the wet sieving, the results were compared and integrated with previous particle size distribution data.

3.2.1 Procedure and Results

The wet sieving procedure used in this work was adapted from ASTM D546, "Sieve Analysis of Mineral Filler for Road and Paving Materials." Minor deviations were made from ASTM D546. These deviations included drying the material at 60°C after sieving instead of 110°C, and using K Basin supernatant instead of tap water as the aqueous fluid. Table 5 lists the Tyler sieve sizes used, along with

the U.S.A. size equivalents and sieve openings. All sieves used in this work were stainless steel and manufactured by W.S. Tyler in conformance to ASTM E11, ANSI, and ISO 565 3310-1 standards.

Table 5. Sieve Sizes Used for Wet Sieving

Tyler Size	U.S.A. Equivalent	Sieve Opening (inches)	Sieve Opening (mm)
5	5	0.157	4.00
12	14	0.0555	1.41
32	35	0.0197	0.500
60	60	0.0098	0.250

The sieve set, nested with the Tyler 5 on top followed by the Tyler 12, Tyler 32, and Tyler 60, was placed on a stainless steel bottom pan equipped with a drain running to a 250-ml or 500-ml receiver jar. The preweighed subsample was rinsed onto the Tyler 5 sieve using K Basin supernatant from the respective sample. K Basin supernatant was then used to rinse as much of the sample as possible through the meshes. A remote video camera, providing color images, was used to inspect the mesh and determine when all particles remaining on the sieve exceeded the mesh size. The sieve was removed, and the material on the next sieve was rinsed in the same manner. All particles that passed through the Tyler 60 sieve either flowed into the receiver jar or were rinsed into the receiver jar at the conclusion of sieving.

Following the rinsing step, the materials retained on each of the sieves were weighed. The mass of wet solids in the receiver was then calculated by subtracting the mass of material in all of the sieves from the original sample mass. A wt% wet solids was calculated for each fraction by dividing the mass of the fraction by the mass of the original sample. Table 6 lists the wt% wet solids separated in each sieve and receiver.

Table 6. Weight Percent Wet Solids Separated by Sieve Size During the Sieving Analysis

Sample	Tyler 5	Tyler 12	Tyler 32	Tyler 60	Receiver
KC-1	0.0	1.0	4.5	5.8	88.7
KC-2/3	0.6	2.2	4.0	15.5	77.7
KC-3	1.7	14.7	12.2	8.4	62.9
KC-4	0.2	0.7	3.4	5.5	90.2
KC-5	1.3	21.2	8.1	5.6	63.8

Table 6 shows that KC-1, collected in the single-pull mode, contains a higher fraction of fine particles than the other canister sludge samples (KC-2/3 and KC-3). It is possible that some fine particulate was lost through the 5-μm filter during the collection of KC-2 and KC-3.

Figures 6 though 10 provide photographs of the material retained on each of the sieves. These figures show that for KC-1 and the KC-2/3 composite, the fine material (<250 μm) passing through the Tyler 60 sieve was dark gray/green in color, while for the remaining samples the fine material was brown. The fine brown material in KC-3 suggests that the fines from KC-2 are responsible for the dark gray color in the KC-2/3 composite.

Green and yellow particles were observed in all of the samples. During work on samples collected from previous KE Basin characterization campaigns, these colors were associated with samples containing high

levels of uranium oxide. Since no analytical work has been performed on the current samples, there is no supporting evidence as to their uranium content.

Sample KC-4 appeared brown prior to sieving. This coloration was the result of fine brown material that was easily washed into the receiver early in the sieving process. The larger particles retained on the sieves were either yellow, green, brown, gray or black.

Sample KC-5 also appeared brown prior to sieving, and the fine brown material was easily washed into the receiver early in the sieving process. Sieving of KC-5 revealed yellow and green particles, possibly indicating the presence of uranium oxide. In addition, organic ion exchange resin beads were found on the Tyler 12, 32, and 60 sieves. Sample KC-5 was collected from a location in the KE Basin that was away from both highly corroded fuel and organic ion exchange beads. Therefore, the presence of yellow/green particles and organic ion exchange resin beads was not anticipated.

Following wet sieving, the sieves and the receiver jars were transferred to a drying oven at 60°C. The materials remained in the oven until a stable mass was reached. The solids retained on the sieves reached a stable mass within the first 24 hours, while the receiver fractions required several days. A wt% dry solids was calculated for each fraction by dividing the dry mass of the fraction by the sum of all of the dry fractions of the respective sample. Table 7 lists the wt% dry solids separated in each sieve and receiver. A comparison of Table 6 with Table 7 shows that, with the exception of sample KC-5, the wet solids profile is similar to the dry solids particle size profile. With KC-5, 36 wt% of the wet solids are >250 μm, while 64 wt% of the dry solids are >250 μm.

Table 7. Weight Percent Dry Solids Separated by Sieve Size During the Sieving Analysis

Sample	Tyler 5	Tyler 12	Tyler 32	Tyler 60	Receiver
KC-1	0.0	1.1	3.5	5.0	90.4
KC-2/3	0.9	3.4	6.0	18.1	71.7
KC-3	3.4	19.8	15.8	8.5	52.4
KC-4	0.2	2.6	5.4	7.4	84.4
KC-5	3.5	35.5	15.4	9.3	36.2

3.2.2 Particle Size Distribution Projections

In a previous report (Bredt et al. 1999), particle size distribution information was compiled for several K Basin sludge streams. This information was collected using a combination of techniques, including sieving (both wet and dry) for particles greater than ~250 μm, and optical instrumentation (Leeds and Northrup Microtrac X100 Particle Size Analyzer and Brinkmann Model 2010 Analyzer) for particles between ~0.12 and 710 μm. From the small-scale wet sieving work conducted here, additional information on the particle size distribution of KE canister and floor sludges has been generated. Since optical instrumentation was not used in the present work, this new information is limited to particles between 250 μm (the smallest sieve used in this work) and 6350 μm (the maximum diameter of the openings in the nozzle of the probe used to sample the sludge from the basin). New information also includes the dry particle density profile as a function of particle size. The previous report (Bredt et al. 1999) assumed uniform density across all particle size ranges. Here, the new particle size data collected during the small-scale wet sieving of the consolidated sludge samples have been combined with the new dry particle density data and with the previously collected optical data to provide a more complete

estimate of the particle size distribution anticipated for the canister and floor sludge waste streams. These estimates are required to predict the volumes of sludge that will result from separation operations to be performed in the K Basin prior to transfer of sludge to T-Plant.

In previous work, canister sludge samples 96-04 and 96-06 were characterized for particle size distribution (Makenas et al. 1997). These samples were designated as "research" samples following settling work, and collected in layers from the settling vessels. Sample 96-04 was divided into an upper (U) and lower (L) layer, while sample 96-06 was divided into an upper (U), middle (M) and lower (L) layer. In most cases, interface layers were also collected (i.e., sample 96-04 U/L is a sample collected at the interface between the upper and lower layers in sample 96-04). Floor sample KES-M-13 was also characterized for particle size distribution in previous work. This sample was also designated as a research sample following settling, and collected in layers from the settling vessel. Sample KES-M-13 was divided into an upper (Top) and lower (Bottom) layer. Layers were uniquely characterized for particle size distribution. In some cases there was insufficient sample to characterize all layers by all techniques.

The wet sieving results for layers from samples 96-04, and 96-06 are presented in Table 8. There was insufficient material to perform wet sieving on the KES-M-13 sample, but a KE floor composite sample (Schmidt et al. 1999) was dry sieved during process development work (results shown in Table 8). This KE floor composite was prepared by combining remaining and archived KE floor samples in proportions that do not necessarily reflect the volumes of sludge in the various areas on the actual KE Basin floor. Although most of the sieving was performed on wet sludge, after sieving the sludge retained on the sieves and receiver was air-dried before weighing. Therefore, the weight percent distributions shown in Table 8 are reported on a dry-sludge basis.

In Figure 11, the sieving results from Table 8 are plotted, along with the sieving results for the consolidated samples from Table 7, as well as results for several other KE Basin samples previously reported. As noted in this figure, three of the consolidated samples (KC-1, KC-2/3, and KC-5) did not compare well with results from previous samples. In the previous analyses, sludge from canisters was found to be relatively coarse material with roughly 50 wt% below 710 μm. Sample KC-3 fits this distribution, but KC-1 and the KC-2/3 composite were much finer, with at least 90 wt% below 500 μm. In addition, previous analyses showed the floor sludge to be fine material with 98 wt% of the material below 500 μm. Sample KC-4 (collected from the floor) compares well with this ≤90% distribution, containing ~92 wt% below 500 μm. However, sample KC-5 (also collected from the floor) is the coarsest material examined, with only 45.5 wt% below 500 μm.

Table 8. Sieving Results from Previous Reports, Wt% Solids Basis (Dry Sludge Basis)

Sample	Method	Tyler 6 (3350 μm)	Tyler 8 (2360 μm)	Tyler 14 (1180 μm)	Tyler 24 (710 μm)	Tyler 32 (500 μm)	Tyler 42 (335 μm)	Tyler 60 (250 μm)	Receiver Pan
KE Floor Comp	Dry	0	0.1	0.2	0.4	0.5	NA	18	81
96-04 L	Wet	0	12	22	9	NA	NA	NA	56
96-06 M	Wet	5	6	20	11	NA	NA	NA	58
96-06 L	Wet	3	3	15	22	NA	NA	NA	58

Table 9 presents the results from previous optical analyses of the canister and floor sludge samples. The optical data are in the form of a cumulative percent (for example, the value of 97.62 in the 44-μm column of 96-04 U/L Sample 1 indicates that 97.62% of the sample volume is composed of particles below 44 μm). For a detailed explanation of the values in Table 9, refer to Bredt et al. (1999).

The particle size distribution calculations were performed to combine the sieving data with the optical data. This calculation was performed by multiplying the vol% data reported from the Microtrac X100 by the mass fraction of material passing through the finest sieve. For example, sample 96-06 M contained 58 wt% (0.58 mass fraction) particles below 710 μm according to sieving data. The Microtrac X100 data (Sample 1) indicate that, of the particles less than ~700 μm, 4.88 vol% of the particles are below 0.972 μm. Therefore, combining the two data sets, the percentage of particles below 0.972 μm is 2.83% (4.88 x 0.58 = 2.83). As stated previously, this calculation is only valid by assuming the density of the particles above 710 μm are the same as the density of the particles below 710 μm. Since wt% and vol% are the same for a sample with uniform density, the results are then both wt% and vol%. On a settled sludge basis, this assumption is generally valid.

Table 9. Optical Particle Size Data from Previous Reports, Vol% Basis

Sample	0.972 μm	5.5 μm	9.25 μm	22 μm	44 μm	104 μm	176 μm
96-04 U/L Sample 1	7.65	50.58	68.94	89.58	97.62	100	100
96-04 U/L Sample 2	0.79	20.12	38.74	72.8	94.05	100	100
96-04 U/L Sample 3	0	8.64	18.24	45.97	70.15	96.07	99.2
96-04 L Sample 1	0	8.24	17.02	41.99	57.92	88.13	94.77
96-04 L Sample 2	3.75	20.44	26.53	39.52	53.56	76.77	85.87
96-06 Carboy	5.55	14.81	24.31	72.04	91.48	100	100
96-06 M Sample 1	4.88	38.18	52.11	69	89	97	99.14
96-06 M Sample 2	1.53	18.75	28.34	47.34	68.81	93.99	98.32
96-06 L Sample 1	8.96	35.54	44.26	60.71	74.59	89.85	94.05
KES-M-13 Top Sample 1	5.23	28.7	44.91	76.07	94.35	100	100
KES-M-13 Top Sample 2	5.25	28.64	44.87	75.86	94.39	100	100
KES-M-13 Bottom Sample 1	3.79	22.31	33.91	56.7	79.01	96.08	99.18
KES-M-13 Bottom Sample 2	3.85	22.27	33.67	55.92	76.89	94.84	98.88

In some cases, sieving data were not available for all the samples analyzed using the Microtrac X100. Sample 96-04 U/L was not sieved, so the 96-04 L sieving results were used for calculations involving sample 96-04 U/L. For calculations involving sample KES-M-13, also not sieved, the KE Floor Comp sieving results were used. Use of the KE Floor Comp sieving results should also reduce errors in sample inhomogeneity, since the KE Floor Comp represents a much larger material mass (~120 g versus 1.5 g of KES-M-13 sieved).

Since samples 96-04, 96-06, and KES-M-13 were split into research layers, average curves were prepared for each of the three samples by combining the research layers in proportion to the estimated volume percent in each layer (see Bredt et al. 1999 for details on this calculation).

No particle size distribution data were available for the upper layers of the KE canister research samples; therefore, the following assumptions were made. For calculation of sample 96-04, the 96-04 U/L layer was assumed to be representative of the upper layer of 96-04. For sample 96-06, the 96-06 Carboy

sample was assumed to be representative of the upper layer of 96-06. Average particle sludge distributions were then calculated for the different sludge types (KE canister sludge and KE floor sludge) using the average sample curves. The particle size distributions for samples 96-04 and 96-06 were averaged to generate an average particle size distribution for KE canister sludge from canisters containing fuel elements, and KES-M-13 was used to determine the average KE floor sludge.

The resulting particle size distributions for the different sludge types are presented in Figure 12. The error bars in these figures indicate the highest and lowest value for each range (high-low bars). A line is used to connect the points, but this line is only provided to guide the eye to the next point and should not be used to interpolate values between points.

As stated above, Figure 12 was calculated using sieving data based on mass and optical data, which are based on volume using the assumption of uniform density across all particle size ranges. Table 13 illustrates that this assumption is reasonable for the floor sludge sample, which had a relatively flat density profile (2.63 to 3.14 g/ml). However, for the canister sludge, the density varied significantly with particle size. For the coarsest particles (400-6350 μm), the density was approximately 2.2 g/ml and increased with decreasing particle size, reaching 7.6 g/ml for the smallest particles (0-250 μm).

The results of the dry particle density analysis were applied to the wt% data in Table 7 to derive particle size distributions based on volume over the entire range. This calculation was performed by assuming that the density profile for KC-2/3 could be applied to samples KC-1, KC-2/3, and KC-3, and that the profile for KC-5 could be applied to KC-4 and KC-5. Since not every size fraction for sample KC-5 was analyzed for density, the value of 2.63 g/ml was applied to the Tyler 5, 12, and 32 fractions; the value of 2.71 g/ml was applied to the Tyler 60 fraction; and the value of 3.14 g/ml was applied to the receiver fraction.

The particle size distributions for samples KC-1, KC-2/3, KC-3, KC-4, and KC-5 are plotted on both a vol% and wt% basis in Figure 13. Figure 13 shows that going from a wt% basis to a vol% basis shifts the curves down. .Therefore, on a vol% basis, there are more larger particles than on a wt% basis. For storage at T-Plant, converting to a vol% basis will increase the size estimate of material in the larger particle fractions (>250 μm).

The sieving data from the consolidated samples, on a wt% basis, were then averaged with the previous samples (curves in Figure 12) to derive average particle size distributions for the different sludge types (KE canister sludge and KE floor sludge). The particle size distributions for samples KC-2/3, KC-3, 96-04, and 96-06 were averaged to generate an average particle size distribution for KE canister sludge from canisters containing fuel elements, and KC-4, KC-5, and KES-M-13 were used to determine the average KE floor sludge. The results are plotted in Figure 14 on a wt% basis.

The dry particle density data were also applied to the data in Figure 12 to convert the previous wt% data to a vol% basis. The results of this calculation are presented in Figure 15. Comparing Figures 12 and 15 shows the curves are pushed downward towards coarser material. As expected, this change is most pronounced in the canister sludge that had a much more significant density change with particle size.

The sieving data from the consolidated samples, on a vol% basis, were then averaged with the curves in Figure 15 to generate a new average particle sludge distribution, also on a vol% basis, for the different sludge types. The results of this calculation are plotted in Figure 16.

Comparing Figure 15 and 16 indicates that, for the canister sludge, the consolidated sludge data pushed the curve up. This is the result of the fine nature of KC-1 and the KC-2/3 composite, as previously noted in Figure 11. The fine nature of KC-1 and the KC-2/3 composite is also the cause of a significant increase in the high-low bars. For the floor sludge, the consolidated sludge data pushed the curve down, and also increased the high-low bars. This change is the result of the coarse nature of the KC-5 sample.

In summary, Figure 12 represents the average particle size distribution data available prior to the consolidated sludge sampling. Figure 12 shows fine particulate floor sludge with approximately 98% of the sludge below 500 μm. Comparing the floor sludge in Figure 12 with Figure 16, the consolidated density profile pushed the vol% curve to a coarser distribution and including samples KC-4 and KC-5 pushed the curve to a significantly more coarse distribution. Figure 12 shows that before the consolidated samples were included the canister sludge was coarser than the floor sludge, with ~58% of the particles below 710 μm. Using the density data to convert to a vol% basis increased the coarse nature of the material, but as Figure 16 shows, this change is minor compared with the influence of the fine nature of KC-1 and the KC-2/3 composite. The result is the fine floor material now appears on average to be coarser than originally considered, and the coarse canister material now appears to be finer. Comparing the floor sludge and the canister sludge in Figure 16 suggests that the floor sludge may contain more particles between 1 and 100 μm. The averages suggest that the floor sludge may also be finer above 100 μm as well; however, there is sufficient variability above 250 μm (indicated by the high-low bars) that the particle size distributions appear roughly the same in this range.

3.3 Large-Scale Wet Sieving

Large samples from KC-4, KC-5, and the KC-2/3 composite were wet sieved through a Tyler 60 mesh, 250-μm openings. This sieving was performed to separate the samples into >250-μm fractions and <250-μm fractions in preparation for process testing. The material >250 μm retained on the sieve is referred to here as "P[plus]250;" and the material passing through the sieves as "M[minus]250" (e.g., the KC-4 material that passed through the sieves is referred to as KC-4 M250, while the material retained on the sieves is referred to as KC-4 P250). In addition to the testing described in this report, the large-scale sieve was also used to prepare test material for large- and small-scale gas generation testing. Note: When the large-scale sieving was conducted, the sludge retrieval plans for KE Basin sludge had the fuel canister and fuel wash sludge split into two streams (>250 μm and <250 μm). These two streams were handled separately; the M250 sludge was combined with the floor sludge, and the P250 canister and fuel sludge was segregated. Since this testing was conducted, the strategy for handling the KE Basin fuel canister and fuel wash sludge is being revised. Under the new evolving strategy, the fuel canister and fuel wash sludge will likely be separated and segregated into streams at 500 μm rather than 250 μm.

The volume of sample for sieving was determined from the volume of each fraction required for the process testing, results from the small-scale sieving, and the volume of material available. Ultimately, 1000 g of KC-4, 50 g of KC-5, and all of the KC-2/3 composite were wet sieved using the Tyler 60 mesh.

Large-scale wet sieving involved placing a portion of a sample on top of the Tyler 60 sieve. The loaded sieve was then raised and lowered repeatedly into a Pyrex pan filled with supernatant taken from the respective shipping canister. As the sieve was raised, particles below 250 μm drained into the Pyrex pan. After the separation appeared complete, the material on the sieve was rinsed with a stream of supernatant from a spray bottle. The runoff from this rinsing went into a 500-ml jar. The material in the 500-ml jar was later combined with the material in the Pyrex pan. The solids on the sieve were immediately transferred to a large vessel filled with clean supernatant to keep the sludge wet at all times. A new

portion of material was then added to the sieve, and this process was repeated until all of the sample was sieved.

3.4 Shear Strength Measurements

Shear strength (τ_s), a semi-quantitative measure of the force required to mobilize the sample, was measured for the M250 and P250 fractions from KC-4 and KC-5 and the M250 fraction of the KC-2/3 composite. The P250 fraction of KC-2/3 did not contain sufficient material. Measurements were made in duplicate with a Haake M5 measuring head electronically remoted for in-cell operation using Technical Procedure 29955-10, "Measurement of Physical and Rheological Properties of Solutions, Slurries and Sludges." Measurements were made at the ambient cell temperature, 33°C.

Since shear strength is dependent on sample history, it was measured after the samples were left undisturbed for approximately 2 weeks. A shear vane, manufactured at PNNL, with the dimensions H_v = 1.582 cm (height) and D_v = 0.800 cm (diameter) was placed in the sample and rotated at a rate of 0.6 rpm. The stress required to maintain the rotational speed was recorded as a function of time. The shear strength was then calculated using the equation below, where 4.9 x 10^5 is the maximum torque of the M5 head and (%τ/100) is the fraction of the total torque, which was recorded as full-scale on the plot of the shear stress.

$$\tau_s = \frac{\frac{\%\tau}{100} x S_\tau x 4.9 x 10^5}{\frac{\pi x H_v x D_v^2}{2} + \frac{\pi x D_v^3}{6}}$$

The measured shear strengths are listed in Table 10. The measured shear strengths for the M250 fractions averaged 2800 dyne/cm^2, while the P250 fractions averaged 28,000 dyne/cm^2. The shear vane used in this testing is not well characterized for the large size of the particles in the P250 fractions; therefore, these data points should be used with caution. [Note: the method and equipment literature does not specify a maximum particle size for a valid shear strength measurement; however, the method was designed to measure the shear strength of fine sands and drilling muds (bentonite clay).] The relative percent difference for duplicate analysis of samples KC-4 M250 and KC-5 M250 was low, 7% and 16%, respectively, indicating good reproducibility. The duplicates for KC-2/3 M250 had a higher relative percent difference, 78%. Only limited KC-2/3 M250 sample was available, and the material in the jar was piled up on one side of it. Therefore, the large difference in duplicate analyses for this sample may be partially attributed to the differences in sludge depths from where the two measurements were performed.

Shear strength information is not just valuable in determining the amount of shear required to mobilize the sludge; it is also valuable in modeling gas retention and release behavior for fine particulate sludge. This gas behavior is an important factor in T-Plant storage. For the samples with larger particles (>250 μm), the shear strength is not dominant in the retention and release mechanism. The pore throats between big particles are large. A relatively low surface tension and large pore throat allows the growing gas bubbles to finger between particles and eventually reach the surface. In this large particle regime,

Table 10. Measured Shear Strengths for Research Layers, dyne/cm^2

Sample	Run 1	Run 2	Average	Relative Percent Difference
KC-2/3 M250	1,700	3,900	2,800	78
KC-4 P250	36,000	20,000	28,000[a]	57
KC-4 M250	3,100	2,900	3,000	7
KC-5 P250	23,000	31,000	27,000[a]	32
KC-5 M250	2,500	2,900	2,700	16

[a] Method is not well characterized for particles of this size.

depending on the dimension of the pore throats and packing of particles, the gas in the sludge will reach some fraction and then be steadily released from the sludge[(a)].

For increasingly smaller particles, the forces preventing fingering of the growing bubble between the particles increase, and gas bubbles are more easily retained. As bubbles grow in these finer materials, the bubbles are forced to displace particles. However, displacement of the particles is hindered by the shear strength of the material. Studies on fine bentonite clays have shown that as the shear strength of the materials increase, bubbles shapes change from round to oblong to slits (Gauglitz et al. 1996). Besides bubble shape, shear strength also affects bubble release mechanisms. For low shear strength materials, the buoyancy of the bubble is enough to overcome the cohesive forces in the material, and bubbles simply rise to the surface. For materials with moderate shear strengths, bubbles are retained until the waste-gas matrix becomes neutrally buoyant. The buoyant mixture then rises to the surface, possibly leading to large and sudden gas release events as observed in Hanford Tank 241-SY-101 prior to mixer pump operations. For high shear strength materials, interconnected slit-shaped bubble networks can form. These networks can provide a mechanism for continuous release.

Between the moderate and high shear strength ranges, vessel-spanning bubbles are possible. This was observed in samples of canister sludge from both KE and K West (KW) Basins (Makenas et al. 1997, 1998). In this regime, the shear strength of the material is not high enough to form a network to the surface, but is high enough to support spanning bubbles. In the case of canister sludge, the spanning bubbles formed in the graduated cylinders containing a layer of settled solids under a layer of liquid. The bubbles pushed up the solids as a plug. If corrective action had not been taken, these spanning bubbles would have forced the liquid, and probably the solids, out the top of the graduated cylinder.

Sample 96-06 was a canister sludge sample from the KE Basin in which spanning bubbles were observed. The shear strengths of 96-06 subsamples were measured between 1700 and 4700 dyne/cm^2. These measurements compare well with the shear strengths measured for the M250 fractions in this work, approximately 2800 dyne/cm^2. Since the samples in this work represent both floor and canister sludges, these results suggest that both types should have a high probability of forming spanning bubbles. Therefore, any storage vessel used in T-Plant should be designed to mitigate the associated hazards. These hazards include flammable gas retention with the possibility of sudden release, and sludge growth

[(a)] The modified Bond number criterion in Gauglitz et al. (1996) is a function of two ratios, gravitational force/surface tension force and pore-scale strength force/surface tension force. With ~200-μm glass beads in water, mostly particle displacing bubbles were observed, while at >500 μm, interstitial liquid displacing bubbles were observed. Therefore a transition at >250 μm is appropriate, especially given the large difference in density between K Basin water (1.00 g/ml) and sludge (2 to >8 g/ml).

that could overrun the storage vessels. Gas retention of any sort will have an adverse effect on the ability of the sludge to transfer heat generated from chemical reactions and radiolysis.

It should also be noted that while the current models would not initially predict the formation of spanning bubbles in the larger particle stream (>250 μm), this could change as the sludge ages. As the sludge ages, the larger particles could oxidize to yield smaller particles. The extent of this change in particle size depends on several factors, including the uranium metal content. If a sufficient fraction of small particles is formed, spanning bubble formation could become a hazard during the T-Plant storage of the large particle fraction.

With respect to gas retention in the large particle sludge, it is important to understand the packing efficiency of the sludge to model the potential gas retention. For both size ranges (<250 and >250 μm), spanning bubbles could be successfully mitigated by vessel design, such as modifying the vessel shape to include a conical taper that prevents the formation of a stable plug.

3.5 Enthalpy Study

Enthalpy tests were conducted to estimate the total metallic uranium content of the P250 fraction of the consolidated sludge samples. The uranium metal content of the sludge is needed to calculate the quantity and rate of heat and hydrogen gas that can be generated from oxidation reactions during sludge transport and storage. The enthalpy data were acquired by dissolving sludge samples in nitric acid in a calibrated adiabatic calorimeter. Dissolution enthalpy data were then used to discriminate between metallic uranium (-3750 J/g in nitric acid) and uranium oxide (-394 J/g in nitric acid). The testing protocols and data reduction methodologies provided in this test procedure were previously employed to determine the enthalpy of dissolution of KW Basin canister sludge (Bredt, P. R., C. H. Delegard, B. M. Thornton, and K. L. Silvers. 1998. *Heat of Reaction in Nitric Acid and Oxidation in Boiling Water of Suspended Metal or Hydride Sludge.* PNNL Letter Report Number 29317-18 to Numatec Hanford Corporation).

The enthalpy of dissolution in nitric acid for the resulting three sieved samples (KC-4 P250, KC-5 P250, and KC-2/KC-3 P250) was examined; the study and results are further described below.

3.5.1 Calorimeter

A calorimeter was assembled as shown in Figure 17. A 100-ml glass beaker cut off at the 80-ml mark was used to contain the 16 M nitric acid. The beaker was wrapped in insulating foam and inserted into a glass vacuum dewar flask. The dewar flask was covered with a piece of foam, and the temperature of the solution in the calorimeter was measured by a mercury thermometer. The thermometer penetrated the foam and into the acid to a fixed depth.

3.5.2 Calorimeter Calibration: System Heat Capacity Determination

The heat capacity of the calorimeter (Cp) was measured by placing a heated stainless steel coupon into the calorimeter and measuring the resulting temperature change. Three measurements of the heat capacity were made. The steel coupons were all heated to 105-107°C. Table 11 lists the results for the heat capacity measurements. It was assumed that the heat capacity for stainless steel was 0.469 J/g-K, and that the heat capacity of the calorimeter and the stainless steel do not change over the temperature

Table 11. Heat Capacity Data for the Calorimeter

Stainless Steel Coupon	Mass (g)	T_2-T_1 (K)	Final Temp. (°C)	Cp (J/K)
SS1	51.6621	7.9	29.2	236
SS1 Dup	51.6621	8.2	32.2	218
SS2	51.7513	7.5	34.7	231
Average				228
Error				7

range examined. Figure 18 plots the temperature of the calorimeter as a function of time for addition of the coupons.

3.5.3 Calorimeter Measurements

Sludge was weighed into a glass thimble and introduced by lifting the foam top, dropping the thimble into the acid, and quickly replacing the foam. The temperature of the calorimeter was then monitored until a stable temperature was reached. The reacted samples were removed from the calorimeter and inspected to determine if the reaction had reached completion. In several cases, gas bubbles were still being generated and released from the sludge, indicating the reaction was not complete. This problem appeared to be caused by the formation of a gel layer on the top layer of sludge in the thimble (see Figures 19 through 21). For samples KC-4 P250 and KC-5 P250, this problem was eliminated by switching to a much wider thimble, which limited the thickness of the gel layer. For sample KC-2/3 P250, changing the sample geometry did not significantly increase the reaction rate, and significant quantities of bubbles were still being generated after the sample was removed from the dewar flask for Test KC-2/3 Dup 2. This is probably due to the presence of uranium metal, which likely did not completely react for the time and temperature of the test. The impact of potentially remaining uranium metal on the enthalpy data is being reviewed. It is expected that issues associated with this data will be resolved before the data are published in the planned SNF characterization report. It may be determined that the enthalpy measurements and uranium metal projections are low for KC-2/3 P250. However, even though the enthalpy values may be low, the presence of significant quantities of uranium metal in sample KC-2/3 P250 is supported by the enthalpy values (discussed later in this section).

3.5.4 Enthalpy of Reaction Calculation

The experiment was conducted in duplicate with samples of KC-4 P250 and KC-5 P250 sludge. The experiment was conducted four times with samples from the P250 fraction of the KC-2/3 composite. Figures 22 through 25 plot the temperature in the calorimeter as a function of time in the addition of the sludge samples. The enthalpy of reaction for the sludge on a wet basis was calculated using Equation 1, while the enthalpy of reaction on a dry basis was calculated using Equation 2. The results and associated data are listed in Table 12.

The relative percent differences for duplicates from samples KC-4 P250 and KC-5 P250 were small, 8% and 34%, respectively, on the dry basis calculations. For sample KC-2/3, four samples were analyzed allowing for the calculation of a 1σ error of ±310 J/g dry or 52% of the average (-596 J/g dry). There is no reason to exclude any of the samples from the data analysis; therefore, it is assumed that the high variability in the KC-2/3 P250 samples is due to problems with obtaining small homogeneous subsamples and incomplete reaction of U metal (i.e., bubbles still observed after termination of the tests).

Table 12. Results for the Heat of Dissolution Calculations

Sample	Mass	T_2-T_1 (K)	ΔH_{wet} (J/g wet)	ΔH_{dry} (J/g dry)
KC-4	1.3917	1.9	-312	-229
KC-4 Dup	2.6663	3.5	-300	-212
Average			-306	-221
Relative % Difference			4%	8%
KC-5	2.778	4.4	-361	-348
KC-5 Dup	1.8205	3.4	-426	-490
Average			-394	-419
Relative % Difference			16%	34%
KC-2/3	0.88	1.4	-363	-345
KC-2/3 Dup	1.4765	4.4	-680	-931
KC-2/3 Dup 2	2.5977	3.9	-343	-315
KC-2/3 Dup 3	2.118	5.6	-603	-793
Average			-497	-596
error (1σ)			170 J/g (34%)	310 J/g (52%)

$$\Delta H_{wet} = \frac{-Cp(T_2 - T_1)}{m} \quad (1)$$

$$\Delta H_{dry} = \frac{-Cp(T_2 - T_1) - \Delta H_d}{m * fs} \quad (2)$$

Where ΔH_{wet} is the enthalpy of reaction for the wet sludge
ΔH_{dry} is the enthalpy of reaction for the dry sludge
Cp is the heat capacity of the calorimeter at constant pressure
T_1 is the initial temperature of the calorimeter
T_2 is the final temperature of the calorimeter
ΔH_d is the heat of dilution for water associated with the wet sludge (values taken from Handbook of Chemistry and Physics, 49th Edition, Linde 1993)
m is the mass of wet sludge
fs is the weight fraction solids (assumed to be 0.5)

3.5.5 Description of Dissolution Chemistry

Uranium metal in the sludge will react with water to generate hydrogen gas. This gas generation could present a flammable gas hazard during sludge collection, shipment operations, and storage at T-Plant. The goal of this enthalpy work was to determine the uranium metal content of the >250-μm sludge particles to bound the potential gas generation hazard. In addition to hydrogen gas, uranium metal also affects how much heat is produced in the sludge.

The heat evolved by dissolution of uranium metal in nitric acid has been calculated based on the enthalpies of formation of the participating reactants and products (Swanson et al. 1985). For the reaction carried out in Hanford reprocessing plant fuel dissolvers

$$U_{(s)} + 5.5\ HNO_{3\,(aq)} \rightarrow UO_2(NO_3)_{2\,(aq)} + 2.25\ NO_{2\,(g)} + 1.25\ NO_{(g)} + 2.75\ H_2O_{(l)}$$

the enthalpy (evolved heat) is -3750 J/g uranium (-213 kcal/mole uranium). Reactions at other product mole ratios are linear combinations of the enthalpies found for pure NO product -4190 J/g uranium (-238 kcal/mole uranium) and pure NO_2 product -3030 J/g uranium (-172 kcal/mole uranium).

The enthalpy of the oxygen-augmented reaction in pilot-plant metal dissolutions

$$U_{(s)} + 4\ HNO_{3\,(aq)} + 2O_{2\,(g)} \rightarrow UO_2(NO_3)_{2\,(aq)} + 2\ NO_{2\,(g)} + 2\ NO_{(g)} + 2\ H_2O_{(l)}$$

was estimated to be -4640 J/g uranium (-264 kcal/mole uranium) and measured to be -4750 ±1060 J/g uranium (-270 ±60 kcal/mole uranium) (Blaine 1960).

Based on published enthalpy of formation data (Wagman et al. 1982), the dissolution of uranium hydride in nitric acid is similarly energetic

$$UH_{3\,(s)} + 11\ HNO_{3\,(aq)} \rightarrow UO_2(NO_3)_{2\,(aq)} + 9\ NO_{2\,(g)} + 7\ H_2O_{(l)}$$

$$UH_{3\,(s)} + 5\ HNO_{3\,(aq)} \rightarrow UO_2(NO_3)_{2\,(aq)} + 3\ NO_{(g)} + 4\ H_2O_{(l)}$$

yielding -3100 J/g uranium (-176.1 kcal/mole uranium) to give NO_2 and -4780 J/g uranium (-271.7 kcal/mole uranium) for NO.

The heats evolved in the dissolution of UO_2 in nitric acid are much lower on a per gram basis than uranium metal and uranium hydride

$$UO_{2\,(s)} + 4\ HNO_{3\,(aq)} \rightarrow UO_2(NO_3)_{2\,(aq)} + 2\ NO_{2\,(g)} + 2\ H_2O_{(l)}$$ -66 J/g UO_2 (-4.2 kcal/mole)

$$UO_{2\,(s)} + 8/3\ HNO_{3\,(aq)} \rightarrow UO_2(NO_3)_{2\,(aq)} + 2/3\ NO_{(g)} + 4/3\ H_2O_{(l)}$$ -394 J/g UO_2 (-25.4 kcal/mole)

The enthalpy of the oxygen-augmented dissolution

$$UO_{2\,(s)} + 3\ HNO_{3\,(aq)} + 1/4\ O_{2\,(g)} \rightarrow UO_2(NO_3)_{2\,(aq)} + NO_{2\,(g)} + 3/2\ H_2O_{(l)}$$

was reported to be -267 J/g UO_2 (-17.2 kcal/mole uranium) (Blaine 1960).

The distribution of the NO_x (NO and NO_2) reaction products in the oxidative dissolution of UO_2 has been shown to be dependent on the acid concentration, temperature, and dilution of the NO_x (Herrmann 1984). This distribution is determined by the equilibrium

$$H_2O_{(aq)} + 3\ NO_{2\,(g)} \leftrightarrow 2\ HNO_{3\,(aq)} + NO_{(g)}$$

For a given HNO_3 concentration, the equilibrium constant expression may be reduced to the equilibrium ratios of the NO and NO_2 partial pressures

$$K_1 = p_{NO}/(p_{NO2})^3$$

A numerical expression for the value of K_1 has been derived based on measurements of the equilibrium between NO_2, NO, and HNO_3 solution at various temperatures and acid concentrations (Tereschenko et al. 1968)

$$\log K_1 = 2.188 \times 10^7 \, T^{-2.58} - 4.571 \times 10^2 \, T^{-1.424} \, c_{HNO3}$$

where T is temperature in Kelvin and c_{HNO3} is nitric acid concentration in weight percent. For the experimental conditions used in the enthalpy measurements, T is about 308 K (35°C) and c_{HNO3} is 70 wt% (16 M HNO_3). Calculating, K_1 is 14.5 atm^{-2}.

It is assumed that the total NO_x pressure in the calorimeter at the end of the reaction is 1 atmosphere. That is, the calorimeter vapor space is filled with NO_x at the end of reaction. This assumption is reasonable given the amounts of sludge used (at least 1 g UO_2), the calorimeter vapor space (60 ml), and the projected amount of NO_x generated (at least 62 ml NO). Thus, $p_{NO2} + p_{NO} = 1$. To satisfy the expression for $K_1 = 14.5$ atm^{-2}, p_{NO2} is calculated to be 0.35 atm and p_{NO} to be 0.65 atm.

The oxidative dissolution of 1 mole of UO_2 to form $UO_2(NO_3)_2$ is a two-electron change. The amount of HNO_3 to be reduced, forming NO_2 and NO, must also be a two-electron change. Reduction of 1 mole of HNO_3 to NO_2 is a one-electron change and to NO is a three-electron change. The amount of HNO_3 required to oxidize 1 mole of UO_2, given the relative amounts of NO_2 and NO, is

$$\text{Moles } HNO_3 = 2 \text{ electrons} / (0.35 \, NO_2 \bullet 1 \text{ electron/mole} + 0.65 \, NO \bullet 3 \text{ electrons/mole}) = 0.87$$

The UO_2 oxidation therefore will require

$$0.87 \bullet 0.35 = 0.30 \text{ moles } NO_2$$

$$\text{and } 0.87 \bullet 0.65 = 0.57 \text{ moles NO}$$

The oxidative dissolution reaction of UO_2 thus is the sum of the two reactions giving, respectively, the specified amounts of NO_2 and NO gas products. Based on the stoichiometries presented earlier for UO_2 oxidative dissolution and the amounts of NO_2 and NO produced in the oxidative dissolution,

$$0.60 \, HNO_3 + 0.15 \, UO_2 \rightarrow 0.15 \, UO_2(NO_3)_2 + 0.30 \, NO_2 + 0.30 \, H_2O$$

and

$$2.27 \, HNO_3 + 0.85 \, UO_2 \rightarrow 0.85 \, UO_2(NO_3)_2 + 0.57 \, NO + 1.14 \, H_2O$$

or, summing,

$$2.87\ HNO_3 + UO_2 \rightarrow UO_2(NO_3)_2 + 0.30\ NO_2 + 0.57\ NO + 1.44\ H_2O$$

The enthalpy of the net reaction to oxidatively dissolve 1 mole of UO_2 is the sum of the enthalpies of the reactions to produce 0.30 moles NO_2 and 0.57 moles NO,

$$0.15\ (-4.2\ \text{kcal/mole}\ UO_2) + 0.85\ (-25.4\ \text{kcal/mole}\ UO_2) = -22.2\ \text{kcal/mole}\ UO_2$$
$$= -366\ \text{J/g}\ UO_2$$

3.5.6 Interpretation of Enthalpy Test Results

The measured enthalpy of reaction for consolidated sludge samples KC2/3 P250, KC-4 P250, and KC-5 P250 was -596, -221 and -419 J/g, respectively, on a dry basis. The value for KC-4 P250 is within the range expected for UO_2, i.e., between -66 and -394 J/g. The value for KC-5 P250 is approximately 15% above the range for UO_2 dissolution. It is possible that a small quantity of the uranium in the sludge is metallic or hydride, resulting in this slightly higher value. The value and observations for KC-2/3 P250 strongly suggest the presence of uranium metal.

The measured enthalpy for two samples from KC-2/3 P250 were -793 J/g and -931 J/g. These values are approximately 2.2 to 2.5 times higher than expected for pure UO_2. Assuming that the material in these samples is only a combination of UO_2 and uranium metal, uranium metal content of the samples can be estimated using the relations,

$$\text{Mass Fraction}\ UO_2\ (366\ \text{J/g}) + \text{Mass Fraction U metal}\ (3750\ \text{J/g}) = \text{Measured Enthalpy J/g}$$

and

$$\text{Mass Fraction}\ UO_2 + \text{Mass Fraction U Metal} = 1,$$

and a uranium metal content of 17.0 wt% and 12.8 wt% for samples KC-2/3 Dup and KC-2/3 Dup 3, respectively, can be estimated. These are conservatively low measurements since not all of the material in the samples was U or UO_2. For example, if 30 wt% of the material in the sample was inert in nitric acid (e.g., SiO_2), the projected uranium metal content for sample KC-2/3 Dup would increase from 17.0 wt% to 24.3 wt%. In addition, the observation that bubbling continued after the samples were removed from the dewar flask indicates the reaction was not complete and, therefore, the measured enthalpy values are biased low.

With respect to storing the sludge at T-Plant, it is probably most appropriate to estimate the uranium metal content by averaging all of the results for sample KC-2/3. Averaging the results limits the errors associated with sample inhomogeneity. Four samples from KC-2/3 were subjected to enthalpy measurements with a total mass of 7.0722 g. Of these four samples, two samples showed no uranium metal, one showed 17.0 wt%, and the last 12.9 wt%. The average was 7.5 (±8.8) wt%.

For KC-5 P250 (measured enthalpy -419 J/g), the calculated uranium metal content was 1.6% on a dry weight basis. Previous analyses of KE floor sludge show that the total uranium content (all uranium compounds) ranges from 3% to 33% on a dry solids basis (Makenas et al. 1996). If it was assumed that 70% of KC-5 P250 was inert (e.g., SiO_2), then the uranium metal content estimated would increase from 1.6 wt% to about 9.1 wt%.

Since the sludge will be recovered and initially stored wet, it is of value to calculate the wt% uranium metal content on a wet basis as well. Two subsamples were collected from the same KC-2/3 P250 settled sludge used for enthalpy testing. The two samples were dried until a stable mass was reached. The dry weights were used to calculate the weight fraction solids in the settled sludge. These results are only applicable to the enthalpy subsamples, since each time subsamples were removed from the bulk sample pots varying amounts of water were added to the pots to prevent drying. Drying of these subsamples yielded weight fraction solids values of 0.51 and 0.57. The average was 0.54. Multiplying the wt% uranium metal on a dry basis (17.0 wt% and 12.9 wt%) by the weight fractions solids (0.54) yields the wt% uranium metal on a wet basis: 9.2 wt% and 7.0 wt%. The average for the four samples was 4.0 (±4.8) wt% uranium metal on a wet basis. Using the weight fraction solids value of 0.43 for KC-5, on a wet solids basis, the uranium metal content for KC-5 is 0.69 wt%.

3.6 Sludge Settling Behavior and Settled Sludge Densities

The settling study was conducted on the solids from samples KC-1, KC-2/3 M250, KC-4, and KC-5. The study on samples KC-2/3, KC-4, and KC-5 was started on October 19, 1999, while the study on KC-1 was started on November 15. For these studies, solids from each sample were transferred into 2-L glass graduated cylinders, 41 cm high and 8.0 cm in diameter. Additional supernatant was transferred into the graduated cylinders to bring the total volume in each cylinder to approximately 1.6 L. Supernatant collected from shipping container KC-5 was used for samples KC-1 and KC-5; supernatant from shipping container KC-2 was used for sample KC-2/3; and supernatant from shipping container KC-4 was used for sample KC-4. The KC-2 supernatant was gray and slightly opaque before being added to the graduated cylinder. The remaining supernatants were clear.

The solids in the graduated cylinders were sparged with inert gas for 10 minutes to mobilize the solid layer and obtain a homogeneous slurry. Ultra high purity N_2 was used for sparging on October 19, and Ar was used on November 15. The volume of settled solids was recorded every 5 minutes for the first half-hour, every 10 minutes for the next half-hour, and then every 20 minutes for the rest of the day. The settled solids volume was then monitored occasionally for the next 2 days. For both studies, a video camera was used to collect real time and time lapse images over the 3-day period. During both sets of settling studies, the cell temperature was approximately 32°C.

For samples KC-1, KC-4, and KC-5, the mobilized solids settled over time, creating a clear liquid layer above and a dark settling slurry layer below. The interface between these layers was monitored as a function of time, and settling velocities were calculated for each. The volume percent settled solids as a function of time are plotted in Figure 26, and the settling velocities as a function of time are plotted in Figure 27. With the exception of sample KC-2/3 M250, all of the samples reached a stable settled volume within the first 4 hours. The supernatant in the graduated cylinder containing sample KC-2/3 M250 remained opaque for the duration of the settling study, so it was not possible to observe the settling behavior.

As seen in Figure 27, the settling rates for samples KC-1, KC-4, and KC-5 were between 0.8 and 1.0 cm/min during the first 30 minutes. After 30 minutes, hindered settling dominated, as indicated by a sharp drop in the settling rate between 30 minutes and 60 minutes. The settling rate for all three samples decreased to approximately 0.03 cm/min after 60 minutes. It is anticipated that in the basin, during fuel and sludge recovery, solids loading will not be high enough to cause hindered settling. Therefore, this study suggests that in the main basin a value of between 0.8 and 1.0 cm/min should be applied. As the

sludge is collected in large quantities in the associated pits and settling tanks, hindered settling will be the dominant settling mechanism. In the pits, a value of 0.03 cm/min or less should be applied.

The results of this study compare with results from the 1996 KE Basin canister sludge campaign (Makenas et al. 1997). During the previous study, an unhindered settling rate of between 0.5 and 3 cm/min was observed. Most of the samples settled within approximately 1 hour, after which the settling velocities decreased rapidly.

The settling rate data for KC-4 and KC-5 are similar to settling data obtained for KE floor and Weasel Pit samples (Makenas et al. 1996). For the KE floor and Weasel Pit samples, settling was essentially complete within 1 to 3 hours (Makenas et al. 1996). During settling tests with single-pull samples conducted in 1999, settling of a composite representative of general KE floor sludge required between 10 and 25 hours [personal communication to D. A. Dodd (Numatec Hanford) from D. B. Bechtold (Numatec Hanford), KE Basin Core Sample Characterization FY 1999 Status, September 20, 1999].

A very different settling behavior was observed during the KW canister sludge campaign, where only three of eight samples were observed to settle with visible interfaces. These samples had settling rates of between 0.04 and 0.02 cm/min; unlike the KE samples, the liquid layer above the interface on these three samples was cloudy. This cloudy liquid took up to 7 days to clear and for one sample never cleared. This settling behavior compares with the behavior of sample KC-2/3 M250 in the present study.

Figure 28 shows the samples following settling. No coarse material was visible in the KC-1 settled solids, and no layered structure was observed. The KC-4 and KC-5 samples settled with a coarse layer on the bottom composed of light-colored chunks and a finer upper layer. In both KC-4 and KC-5, the fine upper layer was a light brown color. These colors match the colors observed for the P250 and M250 fraction separated during the sieving study. The supernatant associated with the KC-2/3 M250 settled solids did not clarify during this study, so the settling behavior over time could not be observed. Figure 28d shows the sample settled with two distinct layers. The upper layer was a light green color, while the bottom layer was a much darker green. Both layers appear to be fine, as would be expected for material sieved through a 250-μm mesh.

Following the settling study, standing supernatant was removed for the graduated cylinders containing the settled solids from samples KC-4, and KC-5. The mass and volume of settled solids was recorded. The settled solids densities were then calculated by dividing the mass by the volume. The density results for all consolidated sludge samples are listed in Table 13.

The settled solids densities for KC-4 and KC-5 agree reasonably well with previous KE floor sludge. The mean settled sludge density of 14 floor sludge samples (Makenas et al. 1996) is 1.32 g/ml (Pearce et al. 1998).

The solids in KC-1 were not weighed in the graduated cylinder. The settled solids were transferred to a 1-L glass jar and re-settled for approximately 2 weeks. Standing liquid was then removed from the jar, and the mass of solids was recorded. The density was then calculated by dividing the mass of settled solids in the jar by the volume of solids in the graduated cylinder before the transfer was made.

Sample KC-2/3 M250 did not contain enough solids to quantify the volume using the 2-L graduated cylinder. The solids from KC-2/3 M250, as well as the solids from KC-2/3 P250, were transferred to 250-μm graduated cylinders and left to settle for approximately 3 weeks. After 3 weeks, the supernatant

above the KC-2/3 P250 solids was slightly cloudy, while the liquid over the KC-2/3 M250 was a dark opaque green-gray. The standing liquid was removed, and the mass and volume of settled solids were recorded. The settled solids densities were then calculated by dividing the mass by the volume.

The average settled sludge density determined for previous KE canister sludge samples (Makenas et al. 1997) was 1.62 g/ml, which is similar to the settled sludge densities determined for KC-1 and KC-2/3. It is interesting to note that for sample KC-2/3, the settled sludge density of the P250 fraction is essentially identical to the M250 fraction.

Table 13. Density of Settled Solids for Consolidated Samples

Sample	Settled Solids Density, g/ml
KC-1	1.488
KC-2/3 M250	2.129
KC-2/3 P250	2.109
KC-4	1.235
KC-5	1.194

3.7 Dry Particle Density

Dried particle densities were measured using a Micromeritics AccuPyc 1330 modified for glovebox operation. This instrument measures the volume of small samples, 0.1-1.0 ml, by exposing the sample to a known pressure of ultra high purity He in a vessel of known volume, and then measuring a pressure drop as the gas is vented to a second vessel of known volume. Samples used for this measurement originated from the small-scale wet sieving work. Following sieving, the samples were dried at 60°C until a stable mass was reached. With the exception of the >250-μm fraction, which contained several inches of standing liquid, stable masses were reached for all samples within the first 24 hours. A weighed portion of the dried solids was placed in the instrument, and the volume was measured. The density was then calculated by dividing the mass by the volume. Due to the high dose rates associated with these dry materials, it was not possible to conduct the analyses in duplicate. Instead, volume measurements were made twice with the same subsample.

The measured dry particle densities are listed in Table 14. For the material from the Tyler 12 sieve of sample KC-2/3, light- and dark-colored particles were observed. Density measurements on this sample were first made on the homogeneous sample, and then on the separated colors. For the remaining samples, particles were too small to be easily separated by color. Therefore, due to the high dose rates associated with the material, the remaining samples were analyzed without any further separation.

The measured density for the light, dark, and mixed particles from the Tyler 12 sieve of sample KC-2/3 were 2.76, 3.21, and 2.89 g/ml, respectively. The mixed sample fell between the separated colors, suggesting that the light and dark fractions have a density difference of ~8%. However, without duplicate analysis, the accuracy of these measurements is unknown.

For sample KC-2/3, a distinct increase in density was seen with decreasing particle size. The dry particle density for the largest particles, 6350-4000 μm, was 2.23 g/ml. The density increased with each range, reaching 7.57 g/ml for the <250-μm fraction. This high density of 7.57 g/ml compares well with measurements of between 7.16 g/ml and 8.04 g/ml made during the K Basin Fuel Subsurface Sludge and

Coatings Characterization effort (Makenas et al. 1999). X-ray diffraction and elemental analysis showed the Subsurface Sludge and Coatings samples were primarily uranium oxide. The specific gravity of uranium oxides is between 8 and 11 (Linde 1993), which suggests that, for sample KC-2/3, the smaller particles (<250 μm) are primarily uranium oxides. It also suggests that the total uranium content (uranium in all phases, metal and oxides) decreases with increasing particle size. Further characterization, including elemental analysis and X-ray diffraction, is needed to support these conclusions.

Table 14. Dry Particle Density for Sieved Fractions from the KE Consolidated Samples

Sample	Fraction	Size Range (μm)	Density (g/ml)
KC-2/3	Tyler 5	6350-4000	2.23
	Tyler 12 Mixed	4000-1410	2.89
	Tyler 12 Light	4000-1410	2.76
	Tyler 12 Dark	4000-1410	3.21
	Tyler 32	1410-500	4.63
	Tyler 60	500-250	6.91
	<250μm	<250	7.57
KC-5	Tyler 32	1410-500	2.63
	Tyler 60	500-250	2.78
	<250μm	<250	3.14

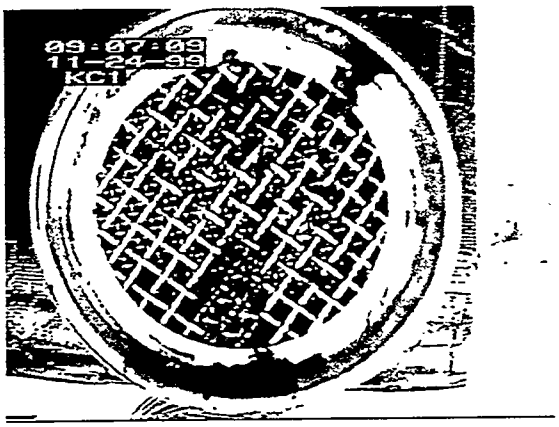

(a)

(b)

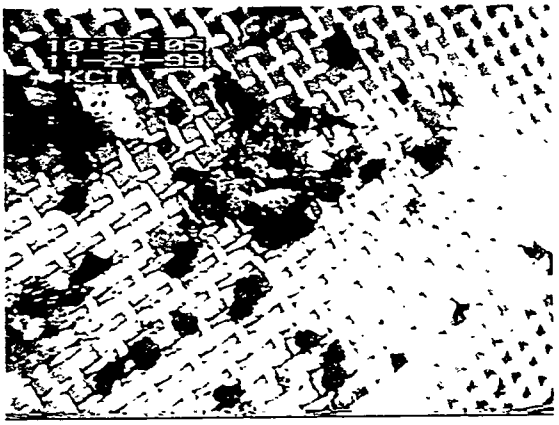

(c)

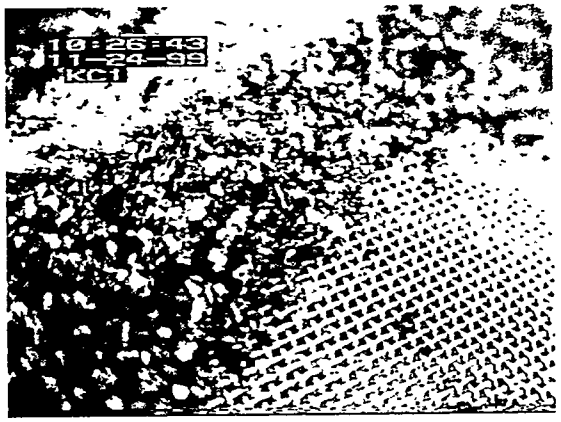

(d)

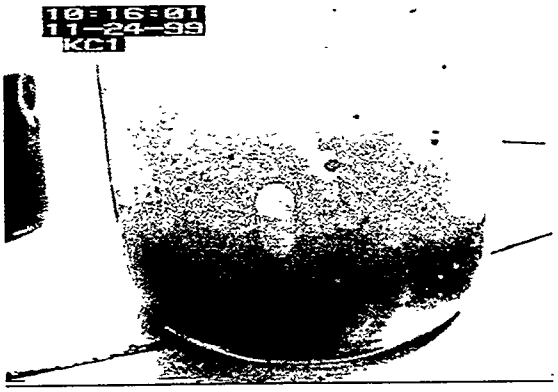

(e)

Figure 6. Small-scale Sieving of Material from KC-1.
(a) no material was retained on the Tyler 5,
(b) through (d) material retained on the Tyler 12, 32 and 60 meshes, respectively, and
(e) <250 μm fraction that passed through the Tyler 60 mesh.

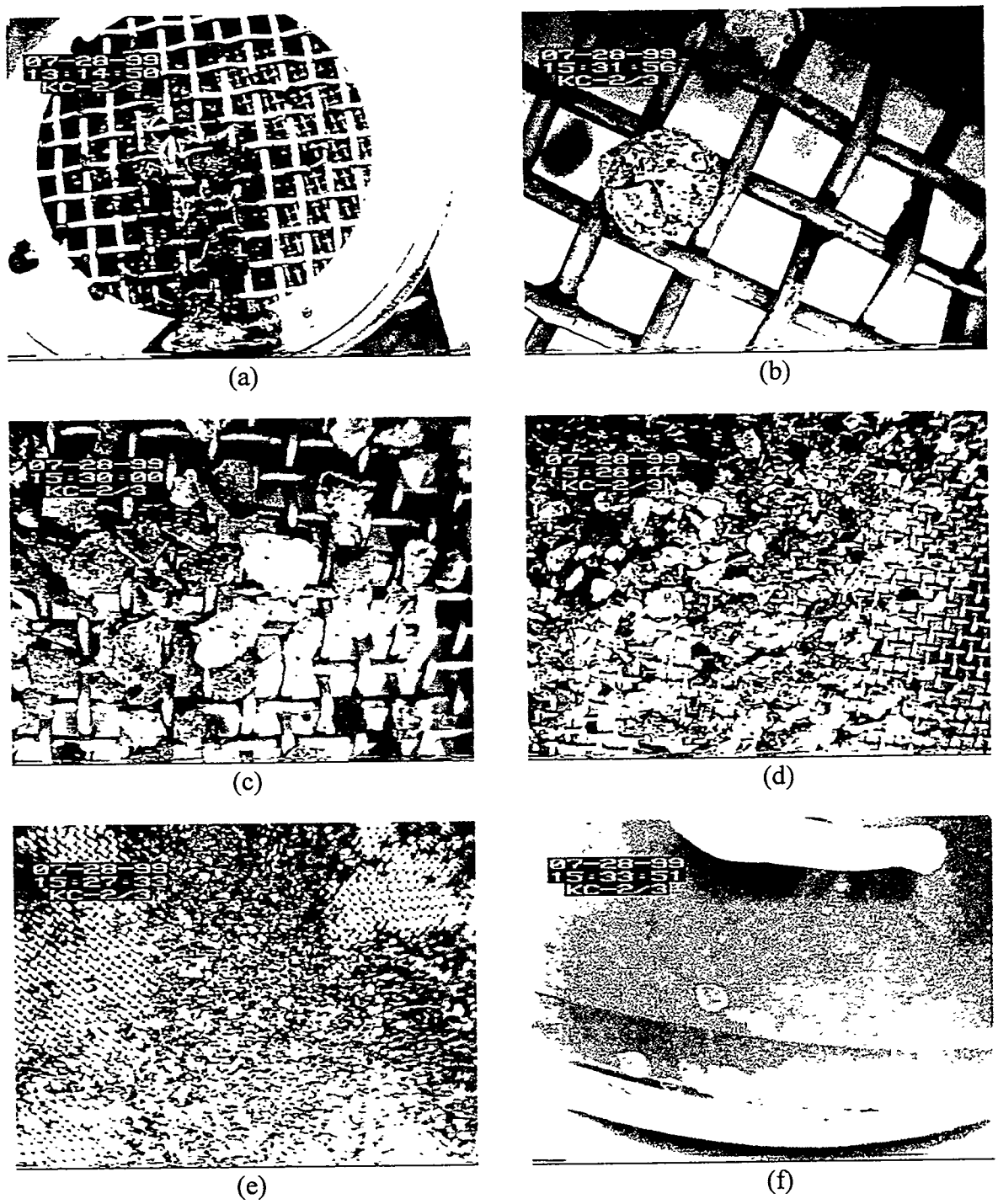

Figure 7. Small-scale Sieving of the KC-2/3 Composite.
(a) material on the sieve stack prior to rinsing,
(b) through (e) material retained on the Tyler 5, 12, 32 and 60 meshes, respectively, and
(f) <250 μm fraction that passed through the Tyler 60 mesh.

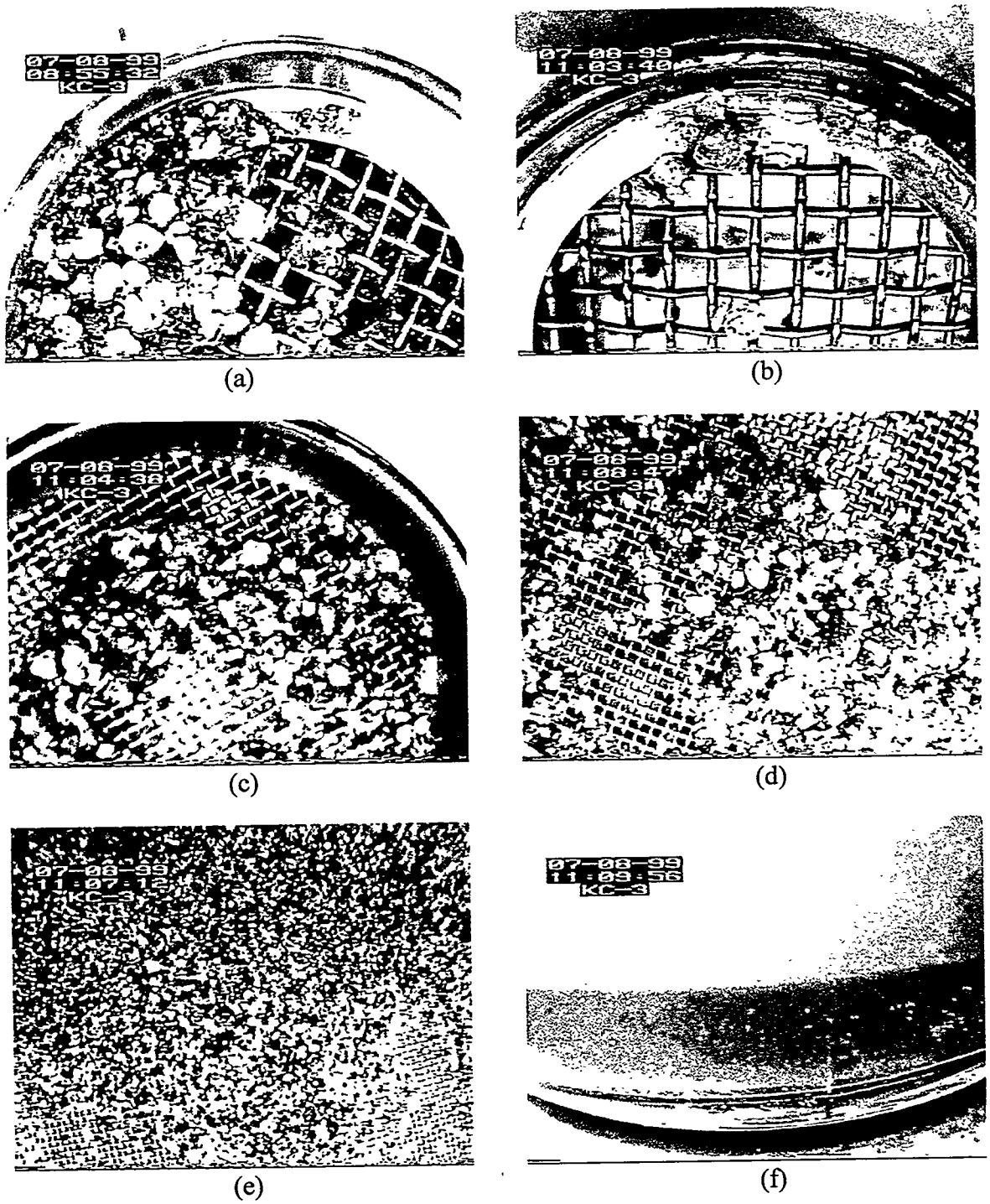

Figure 8. Small-scale Sieving of Material from Canister KC-3.
(a) material on the sieve stack prior to rinsing,
(b) through (e) material retained on the Tyler 5, 12, 32 and 60 meshes, respectively, and
(f) <250 μm fraction that passed through the Tyler 60 mesh.

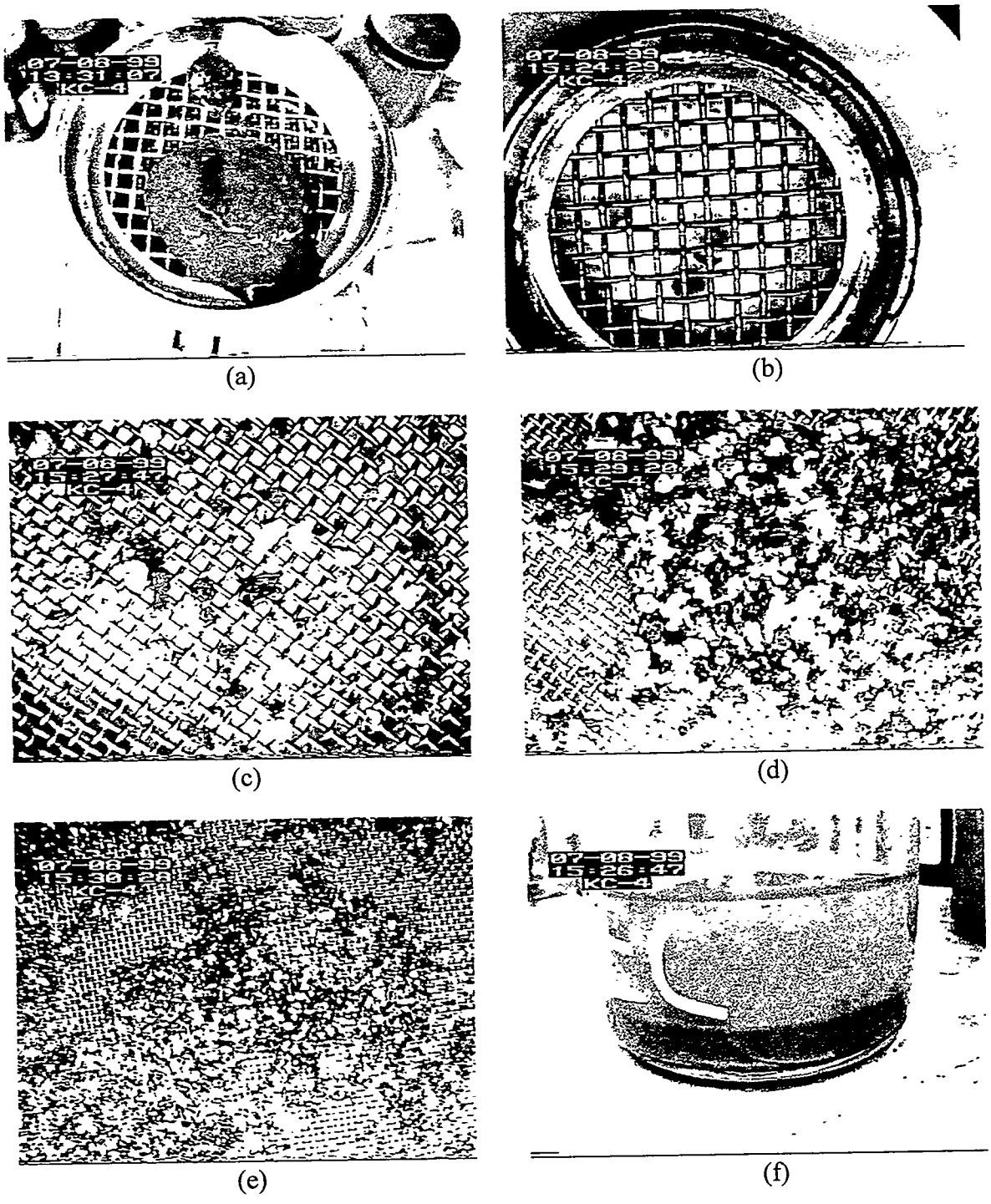

Figure 9. Small-scale Sieving of Material from Canister KC-4.
(a) material on the sieve stack prior to rinsing,
(b) through (e) material retained on the Tyler 5, 12, 32 and 60 meshes, respectively, and
(f) <250 μm fraction that passed through the Tyler 60 mesh.

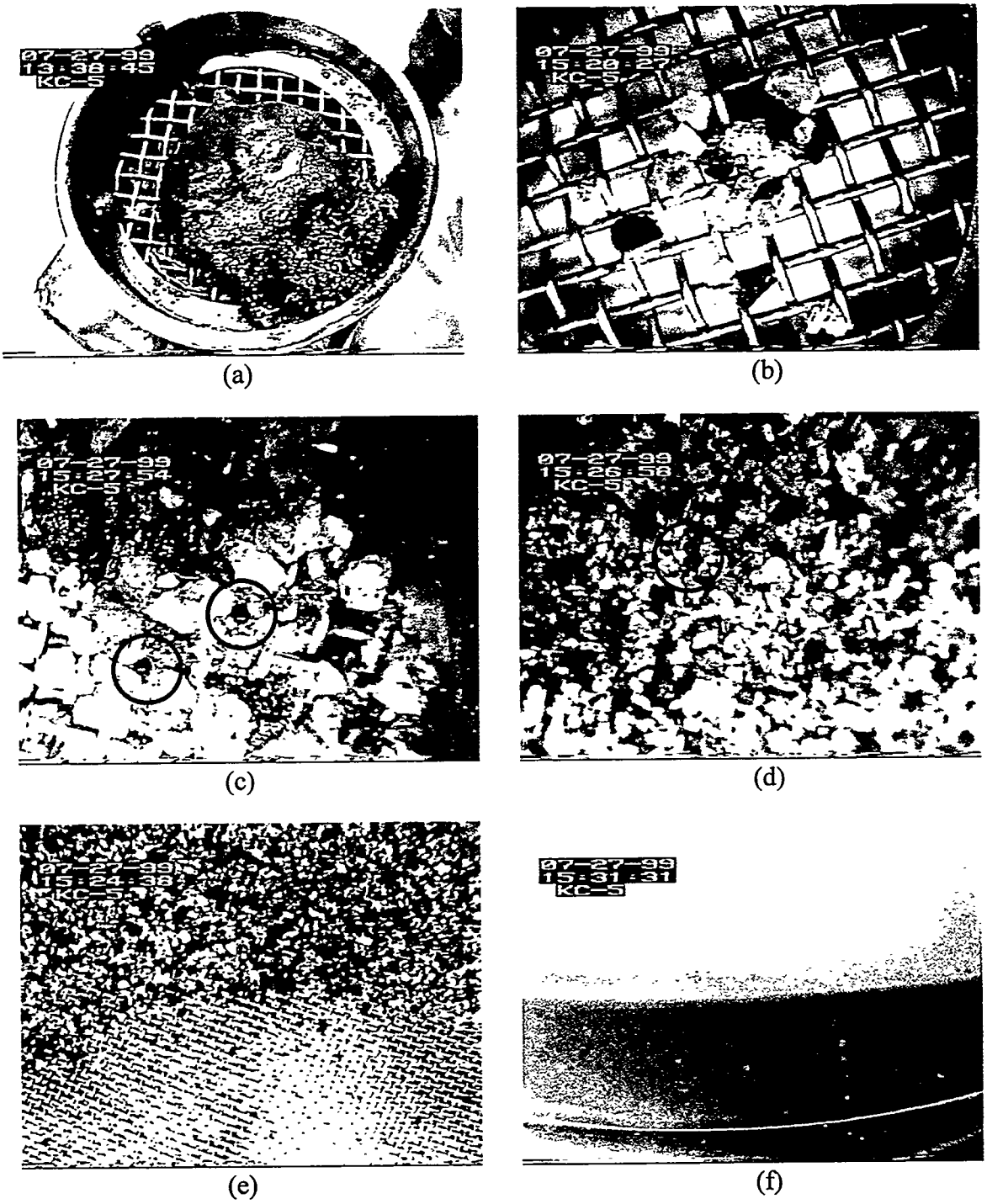

Figure 10. Small-scale Sieving of Material from Canister KC-5.
(a) material on the sieve stack prior to rinsing,
(b) through (e) material retained on the Tyler 5, 12, 32 and 60 meshes, respectively. Several organic ion exchange beads are circled in (c) and (d), and
(f) <250 μm fraction that passed through the Tyler 60 mesh.

Figure 11. Comparison of Sieving Results for K East Basin Sludges and Consolidated Sludge on a Dry Weight Basis

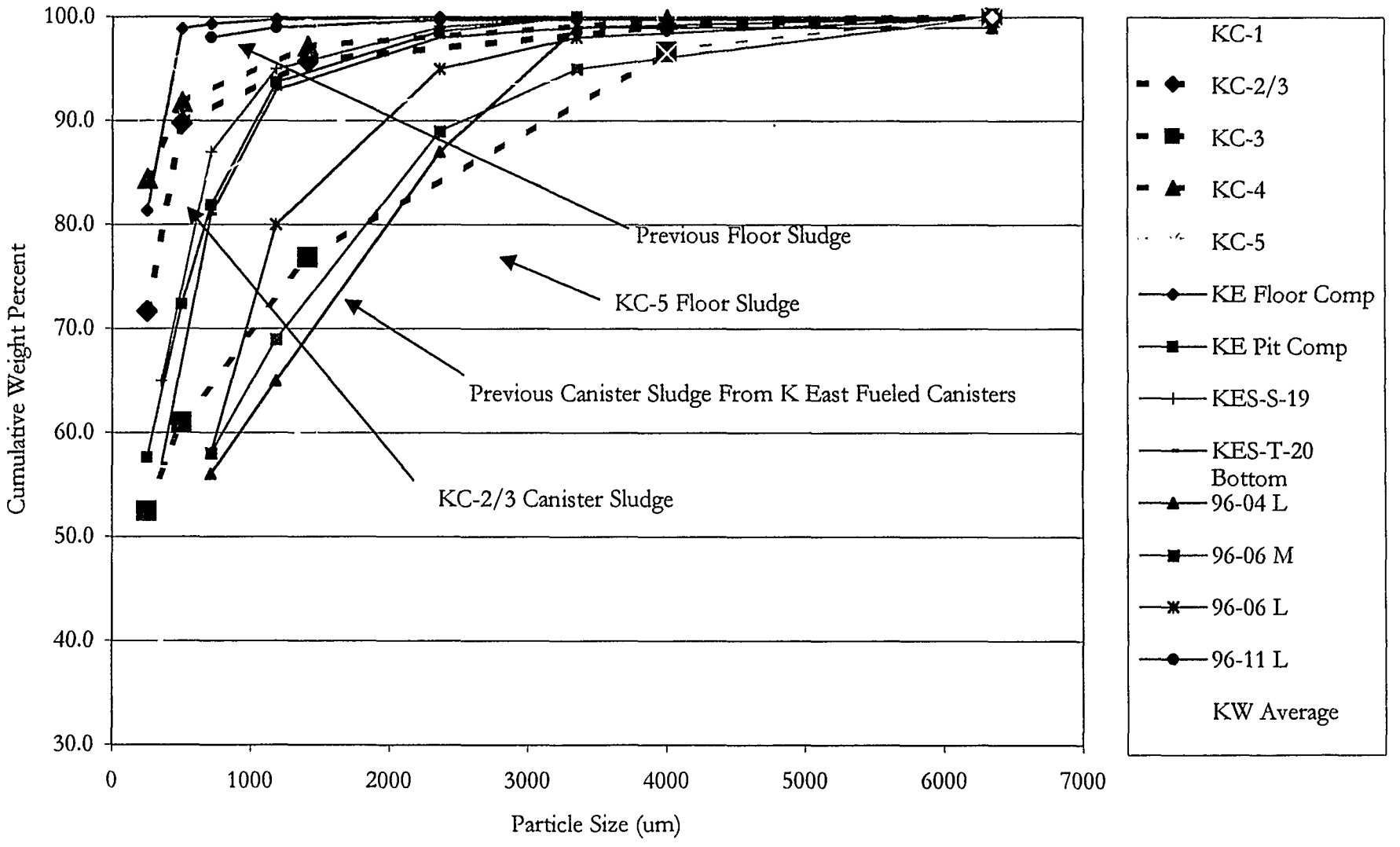

Figure 12. Weight Percent Particle Size Distribution for K East Fueled Canister and Floor Sludge Without Consolidated Sludge Samples

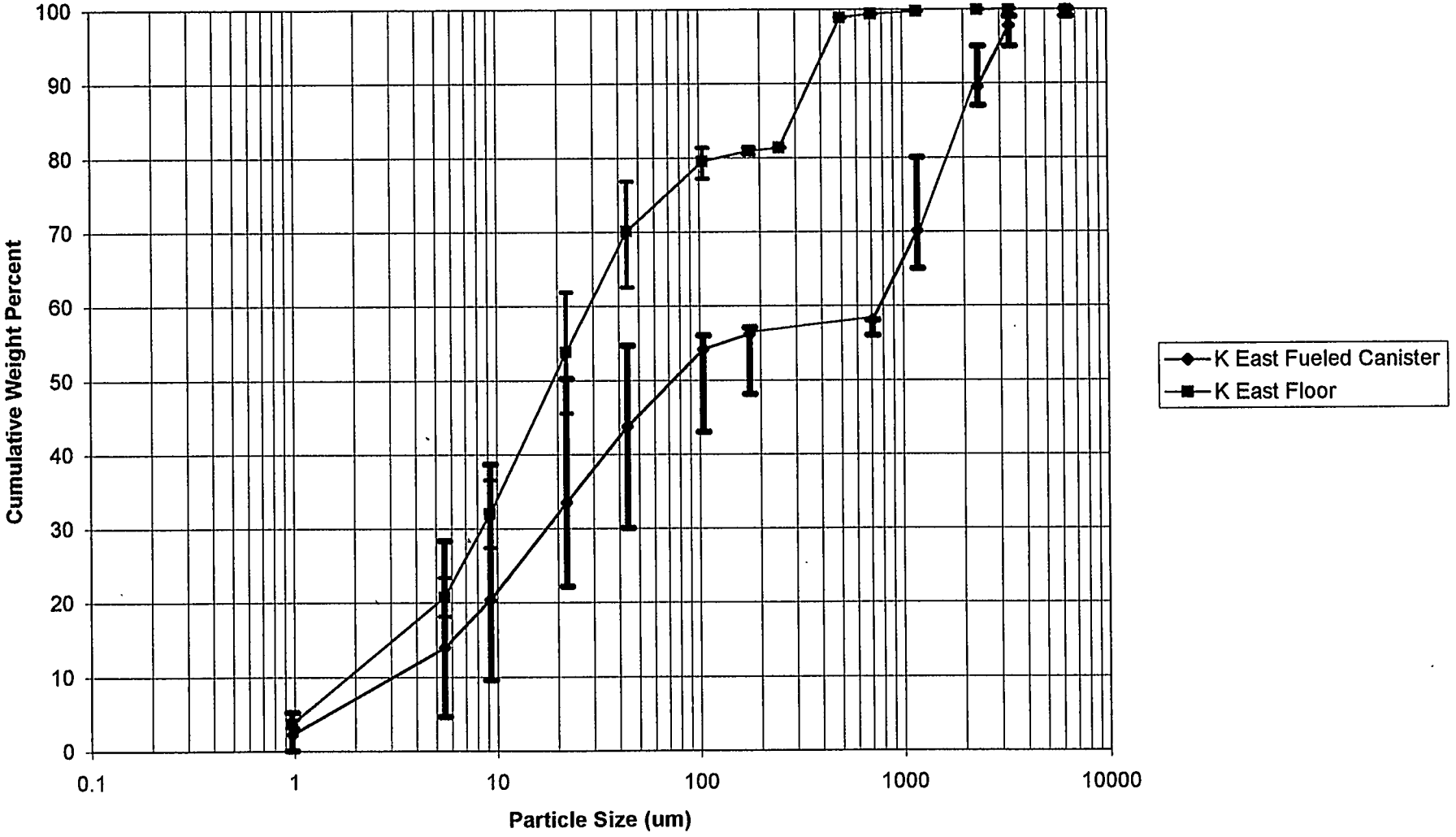

Figure 13. Comparison of Volume Percent and Weight Percent Particle Size Distributions for K East Basin Consolidated Samples

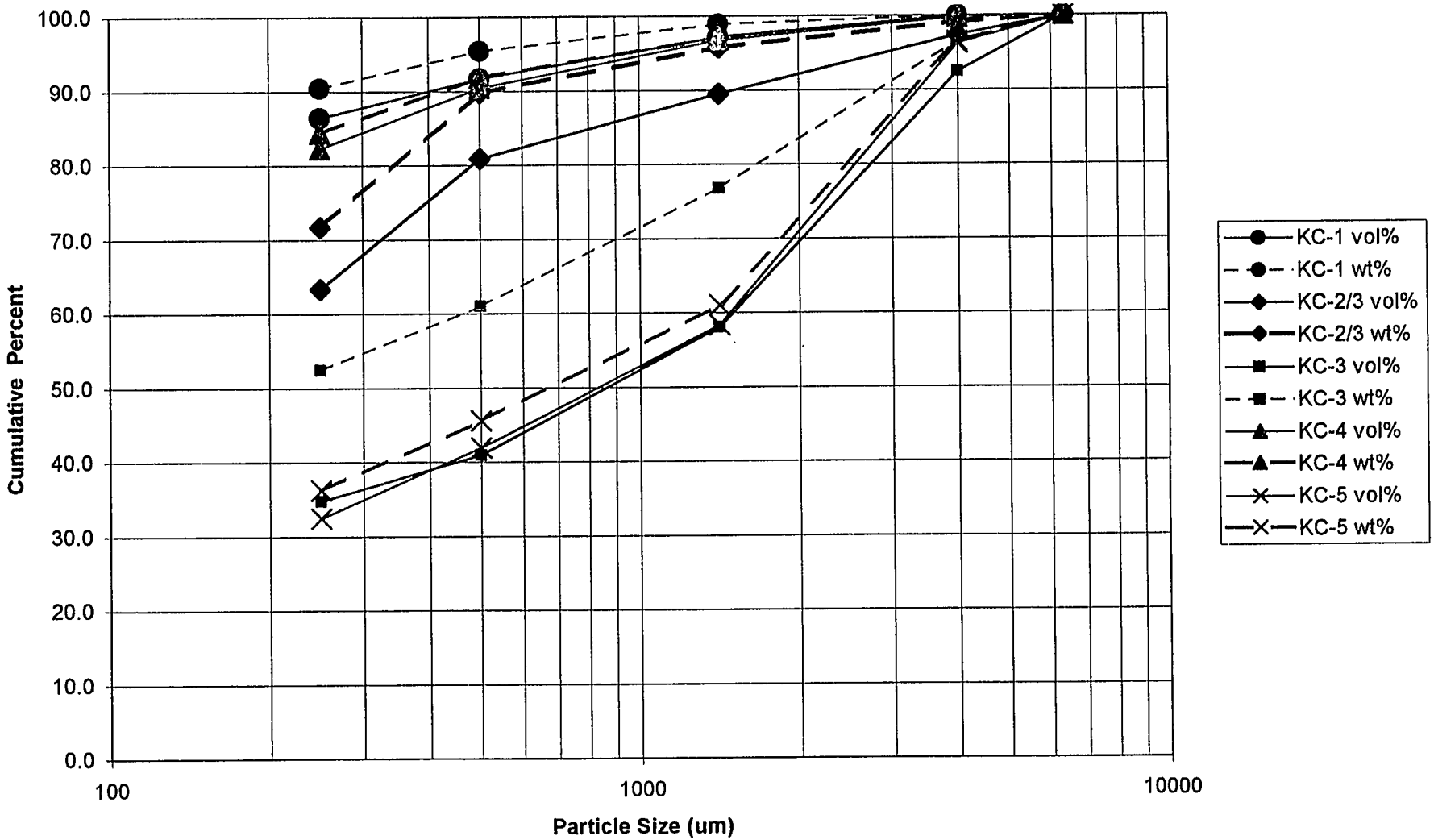

Figure 14. Weight Percent Particle Size Distribution for K East Fueled Canister and Floor Sludge Including Consolidated Sludge Samples

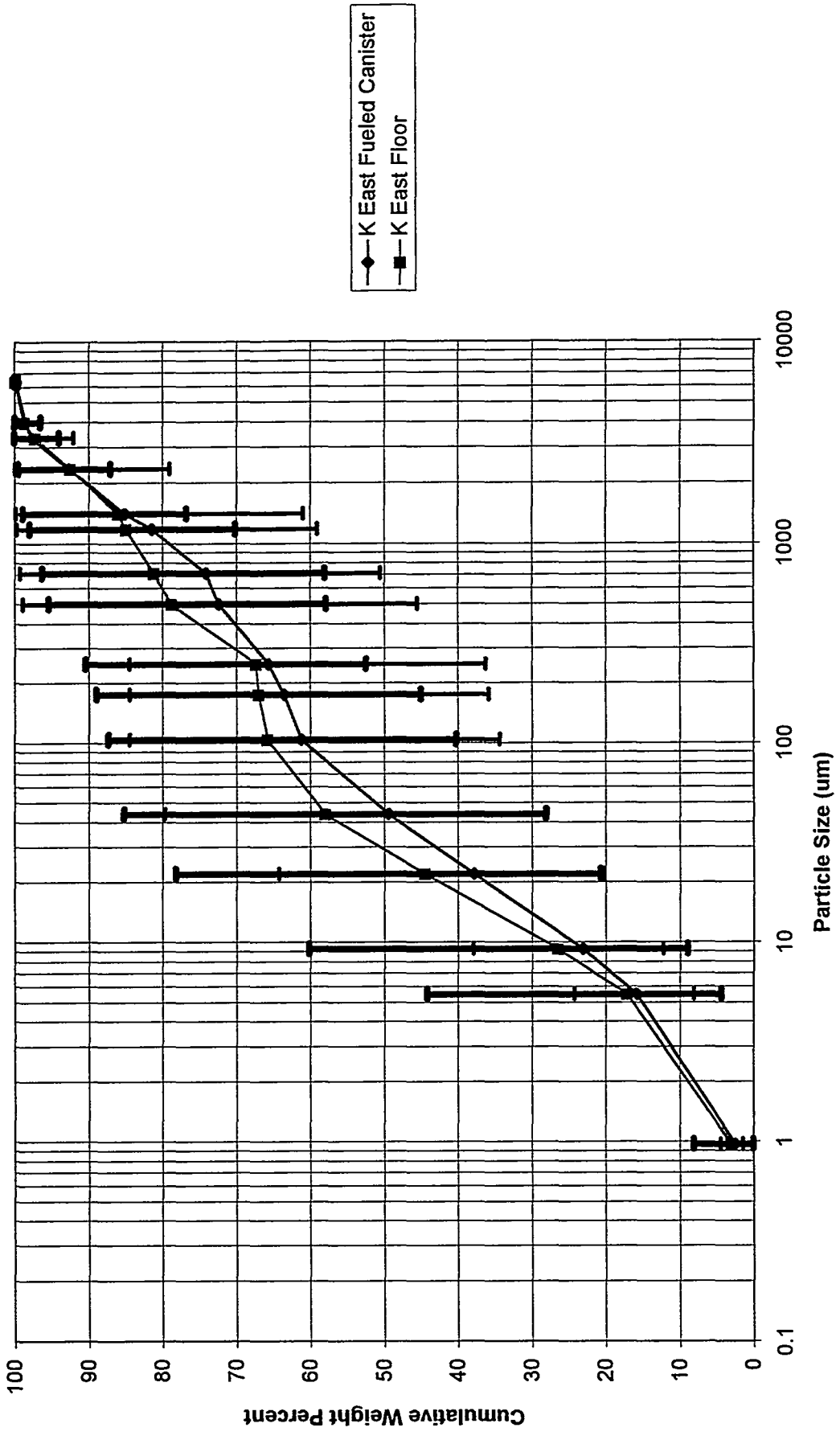

Figure 15. Volume Percent Particle Size Distribution for K East Fueled Canister and Floor Sludge Without Consolidated Sludge Samples

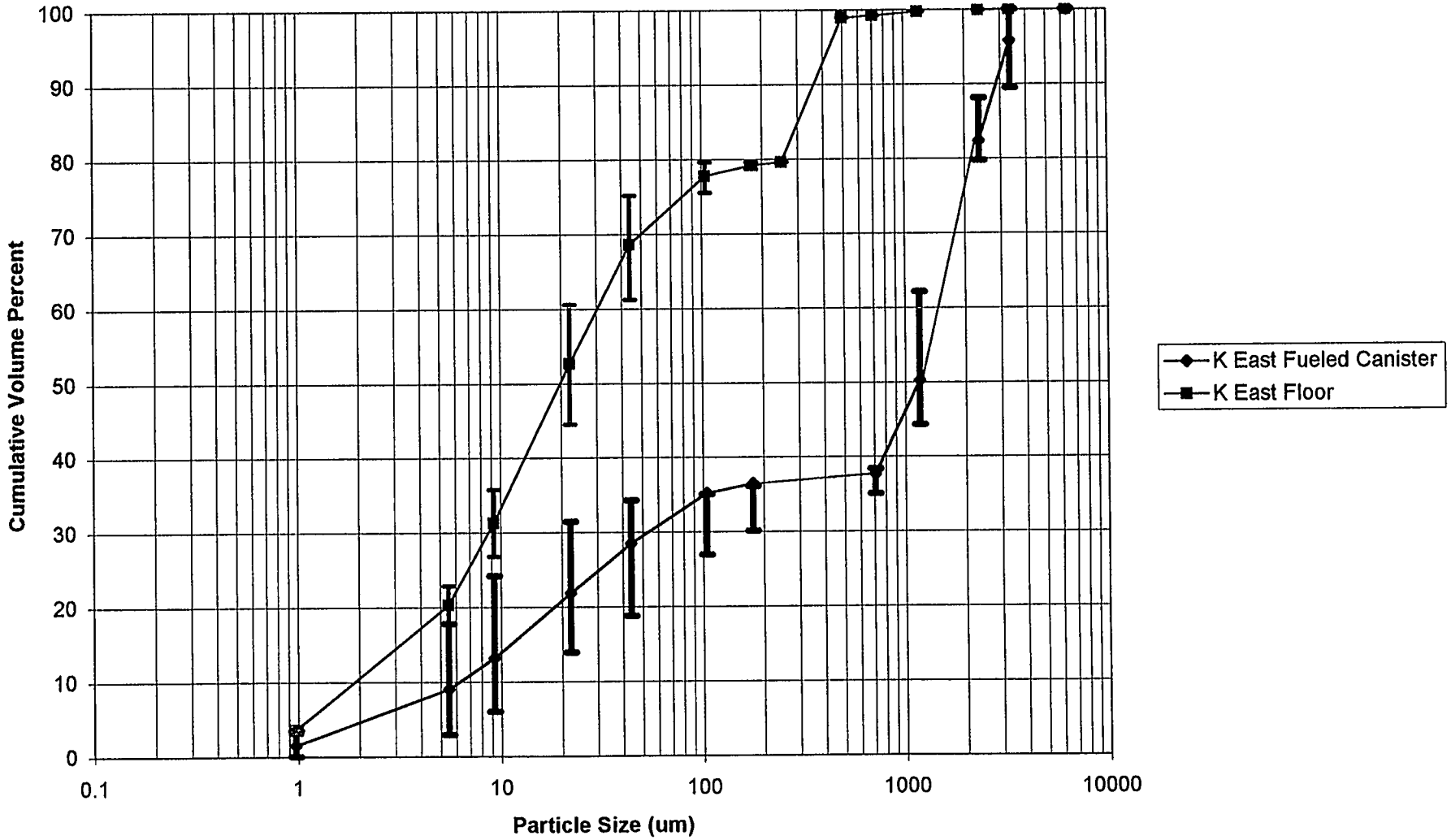

Figure 16. Volume Percent Particle Size Distribution for K East Fueled Canister and Floor Sludge Including Consolidated Sludge Samples

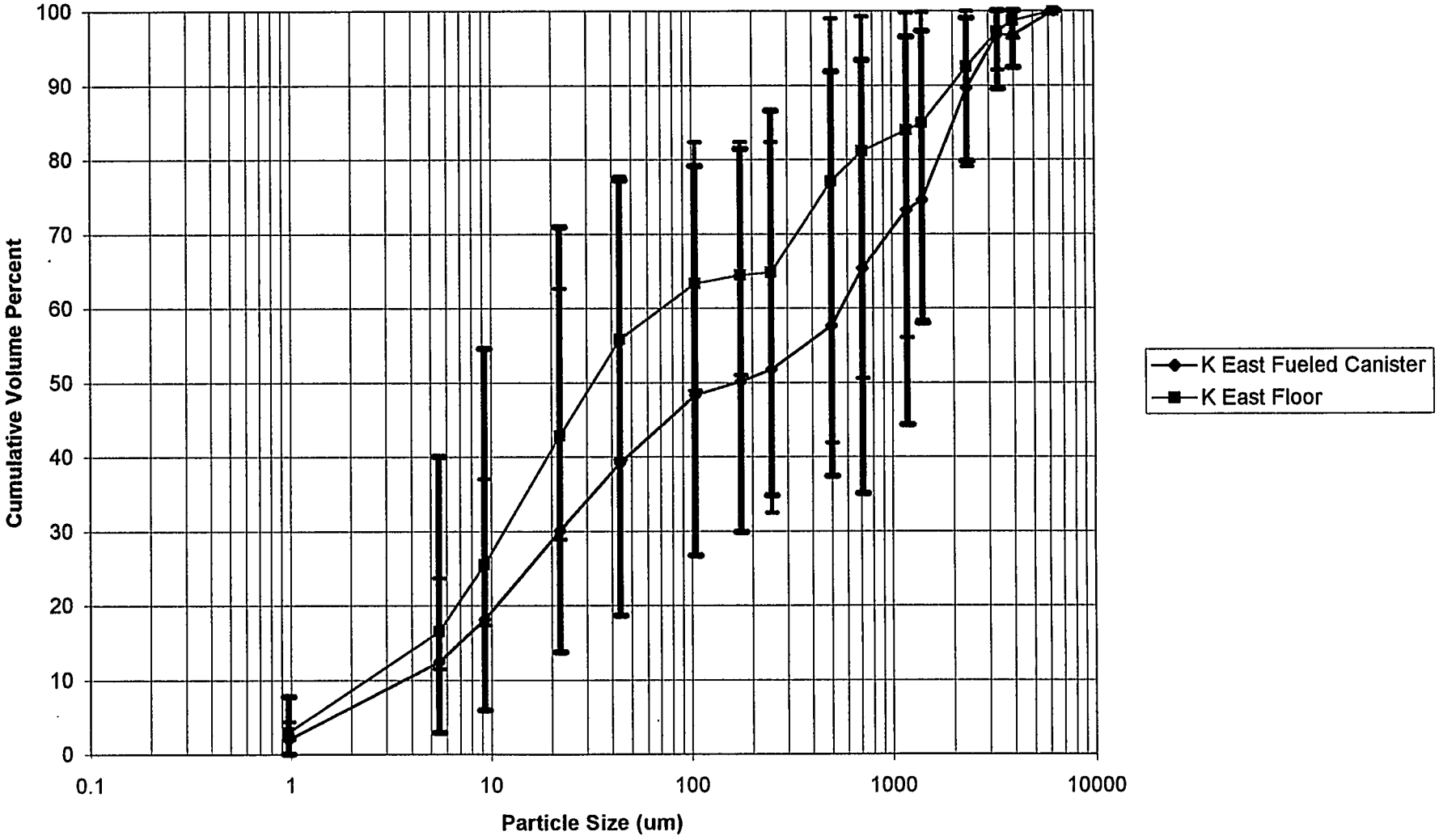

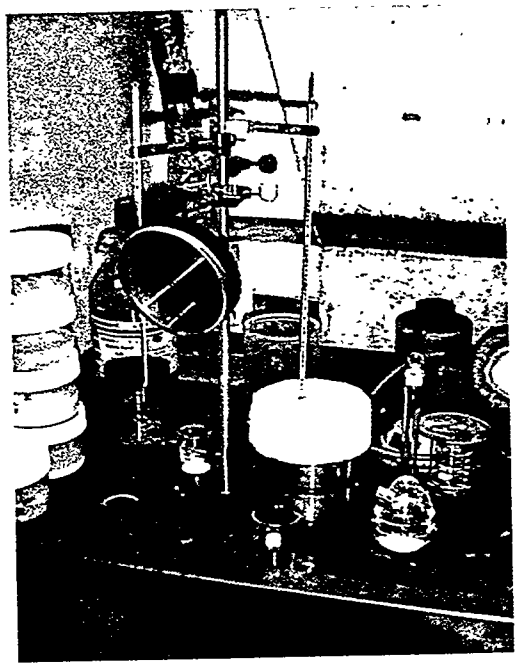

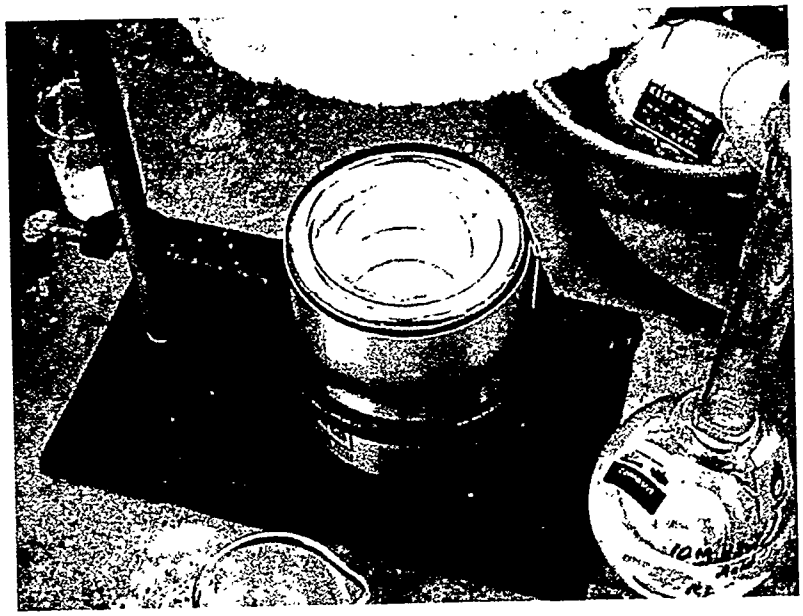

Figure 17. Calorimeter in the Fume Hood During Calibration

Figure 18. Temperature Versus Time for Addition of Stainless Steel Coupons to Calorimeter

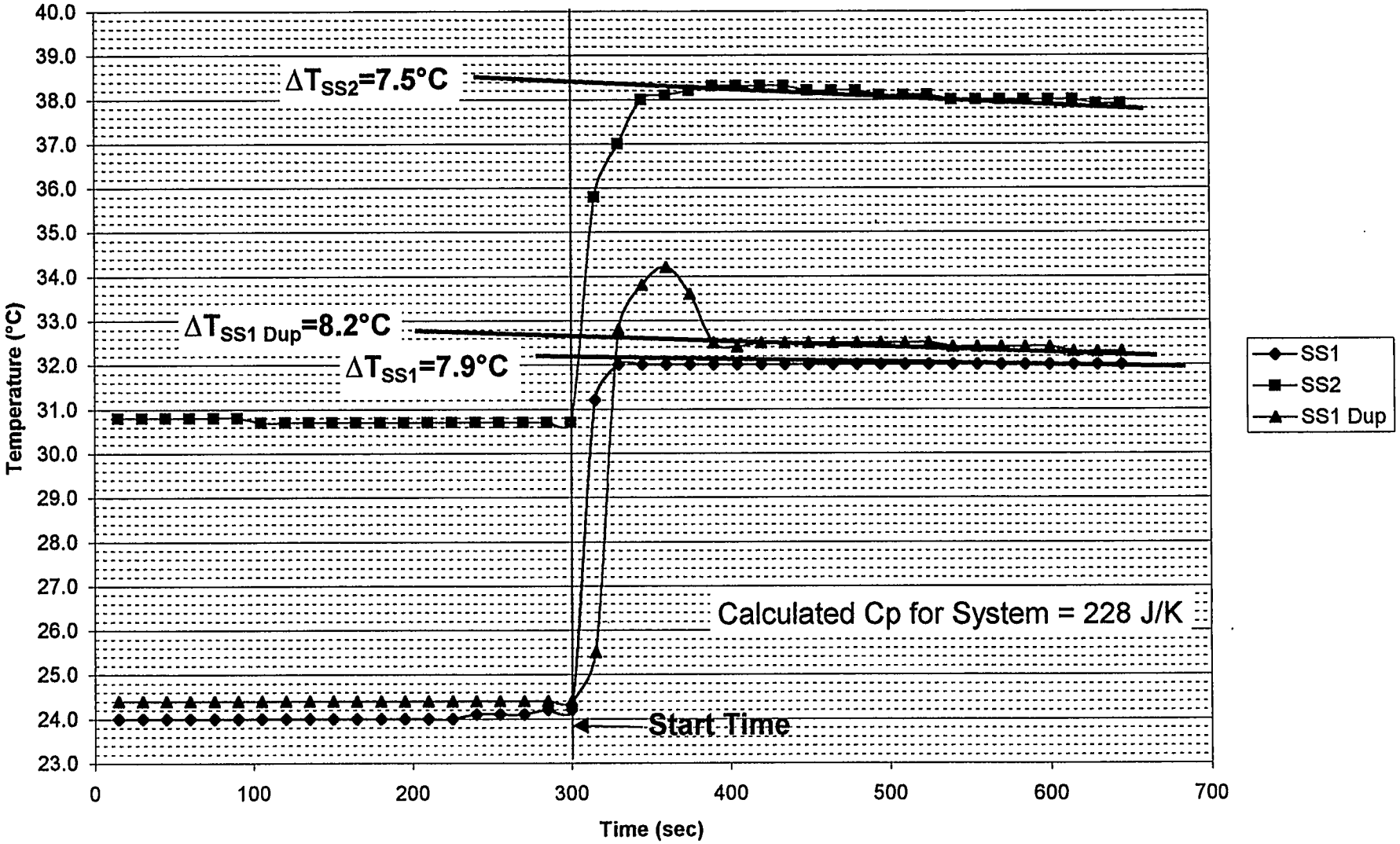

Note: The temperature excursion on SS1 Dup was the result of the thermometer initially being located too close to the heated stainless steel coupon. Upon noticing the excursion, the thermometer was moved to give a more accurate measure of the bulk solution temperature.

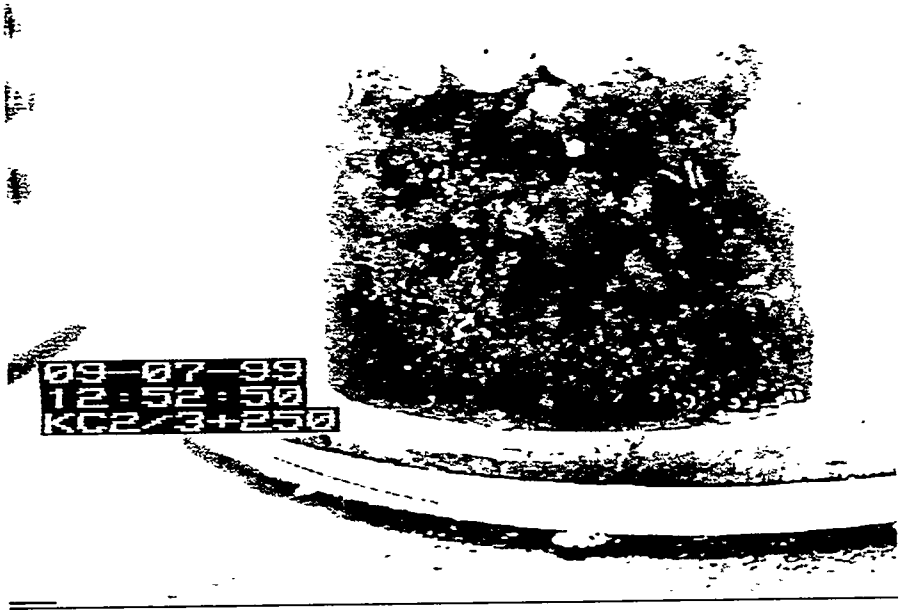

(a)

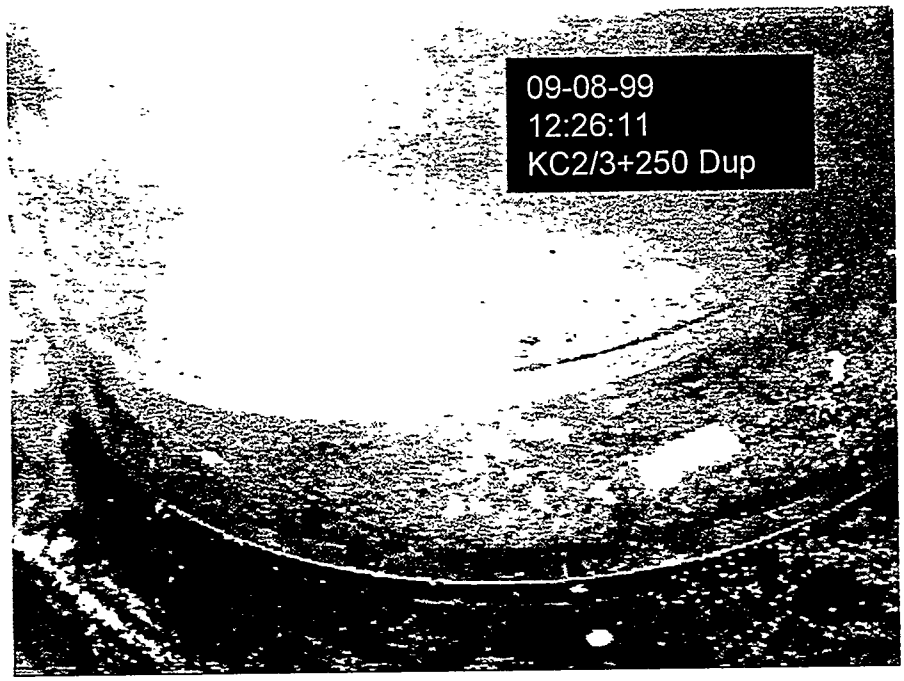

(b)

Figure 19. Insoluble Residue from the >250 μm Fraction of the KC-2/3 Sludge Composite After Treatment in 16 M Nitric Acid at ~25°C.
(a) shows sludge remained in the thimble following dissolution and some unreacted sludge may be trapped at the bottom, while
(b) shows sludge was ejected from the thimble and well reacted.

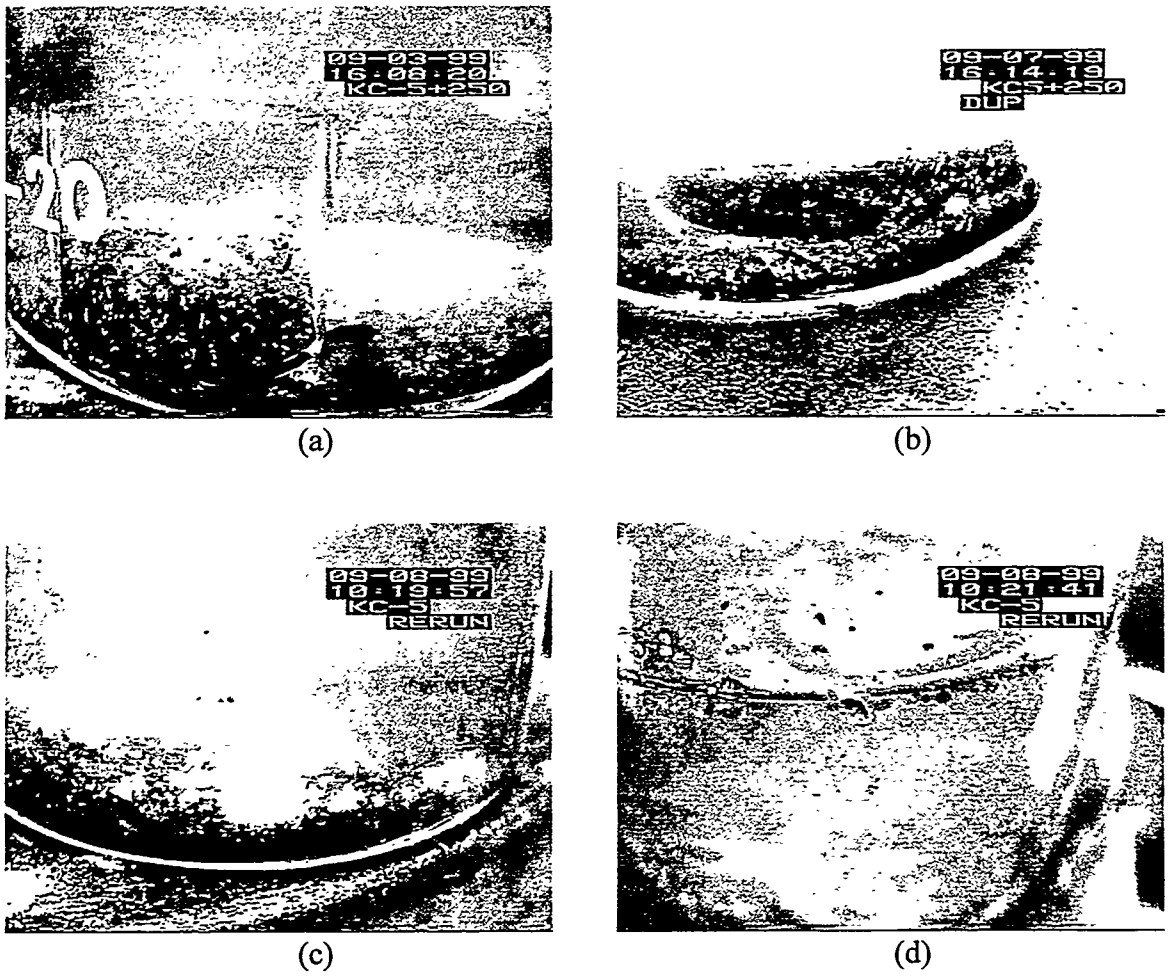

Figure 20. Insoluble Residue from the >250 μm Fraction of KC-5 After Reaction with 16 M Nitric Acid at ~25°C.
(a) shows unreacted black material trapped under a light colored layer (probably silicate gel); bubbles are continually released as the black material reacts with the acid.
(b) and (c) show duplicate samples analyzed using a wider thimble with no unreacted sludge.
(d) shows organic ion exchange resin floating on top of the acid following analysis of the third sample; organic ion exchange resin was observed following all three KC-5+250 μm analyses.

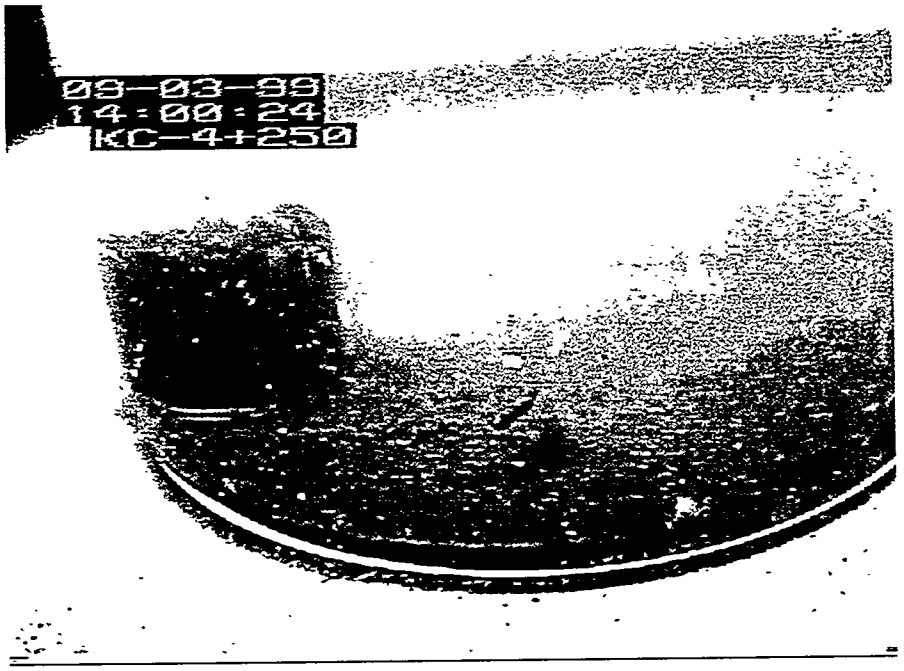

(a)

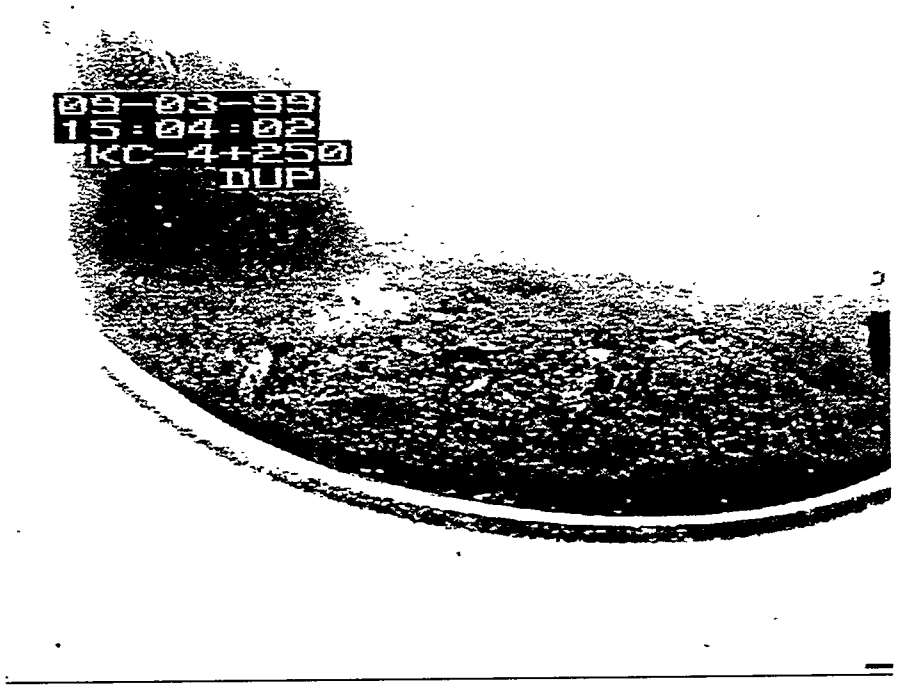

(b)

Figure 21. Insoluble Residue from the >250-μm Fraction of the KC-4 Sludge Composite After Treatment in 16 M Nitric Acid at ~25°C. Both photographs show approximately 50% of the sludge remained in the thimble following dissolution but no evidence of unreacted sludge.

Figure 22. Temperature Versus Time for Dissolution of Samples from KC-4 P250

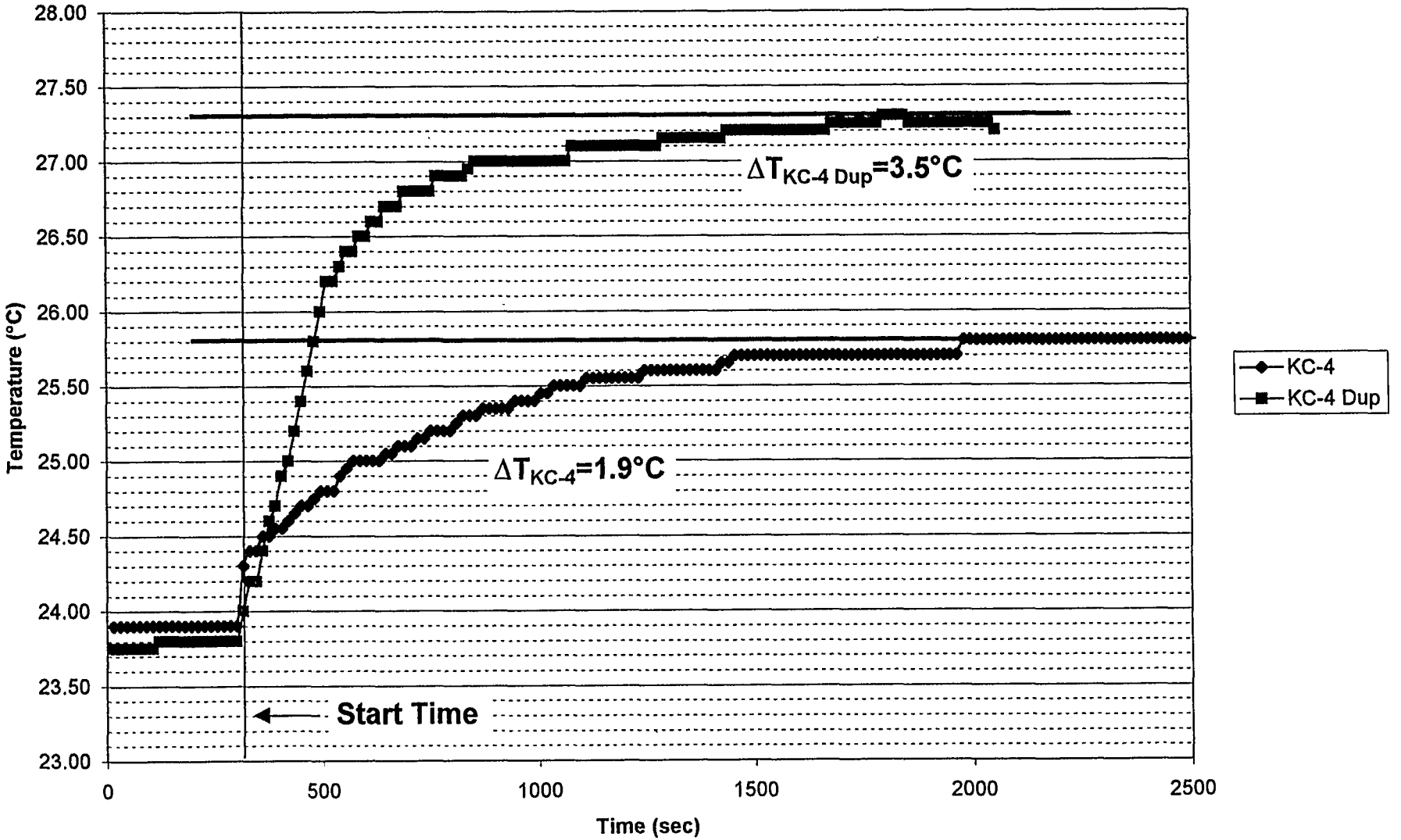

Figure 23. Temperature Versus Time for Dissolution of Samples from KC-5 P250

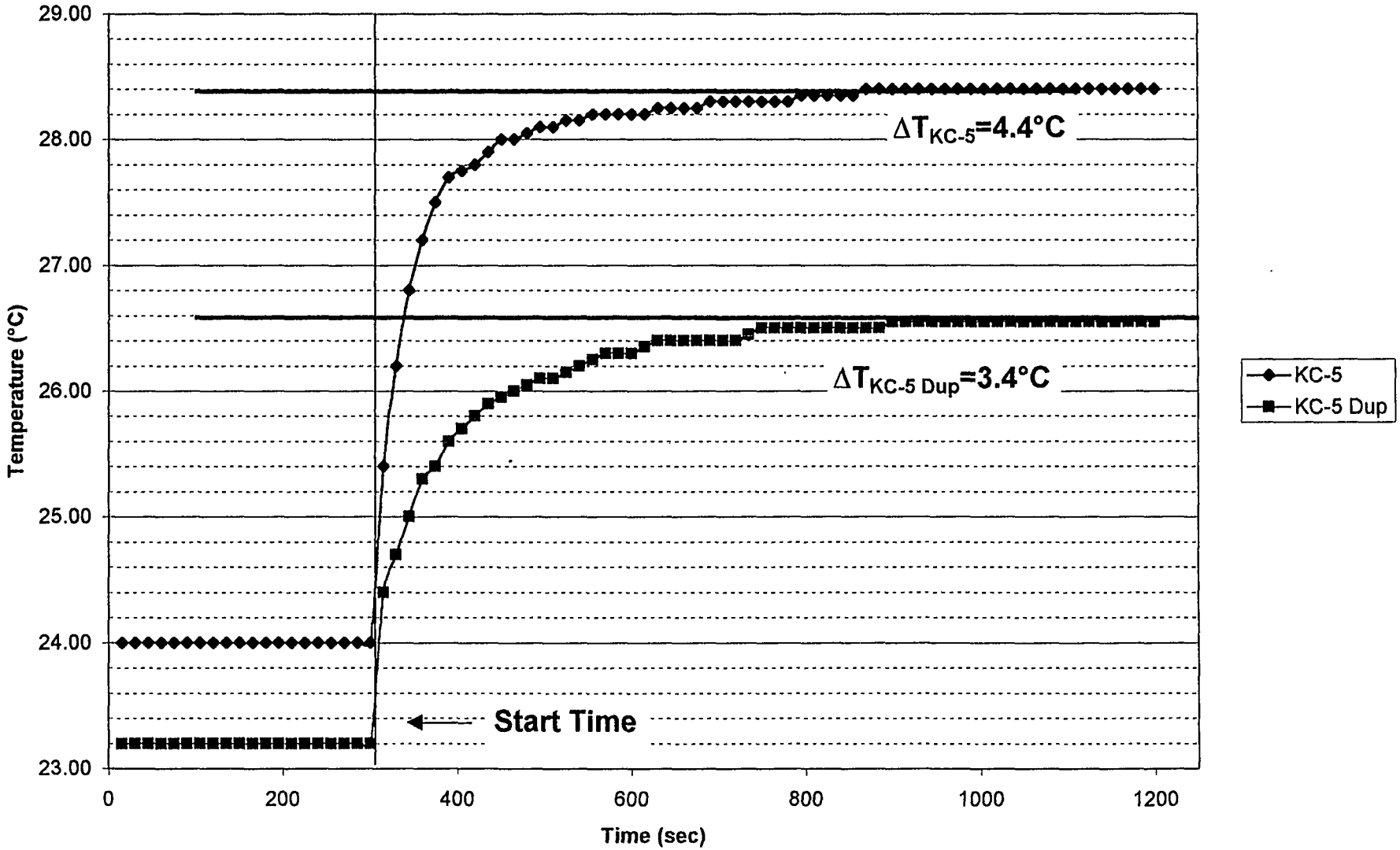

Figure 24. Temperature Versus Time for Dissolution for First Two Samples from KC-2/3 P250

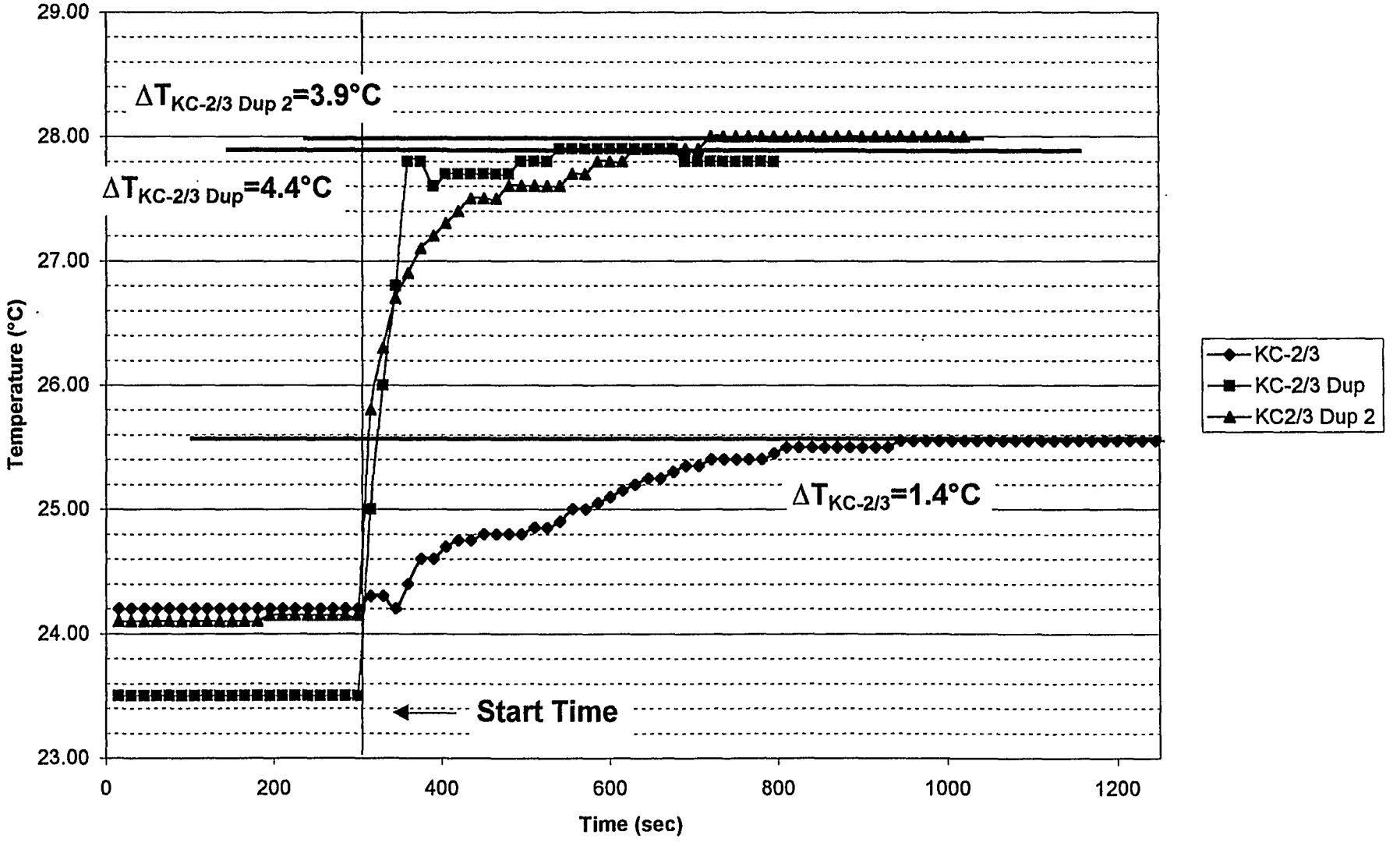

Figure 25. Temperature Versus Time for Dissolution of Final Sample from KC-2/3 P250

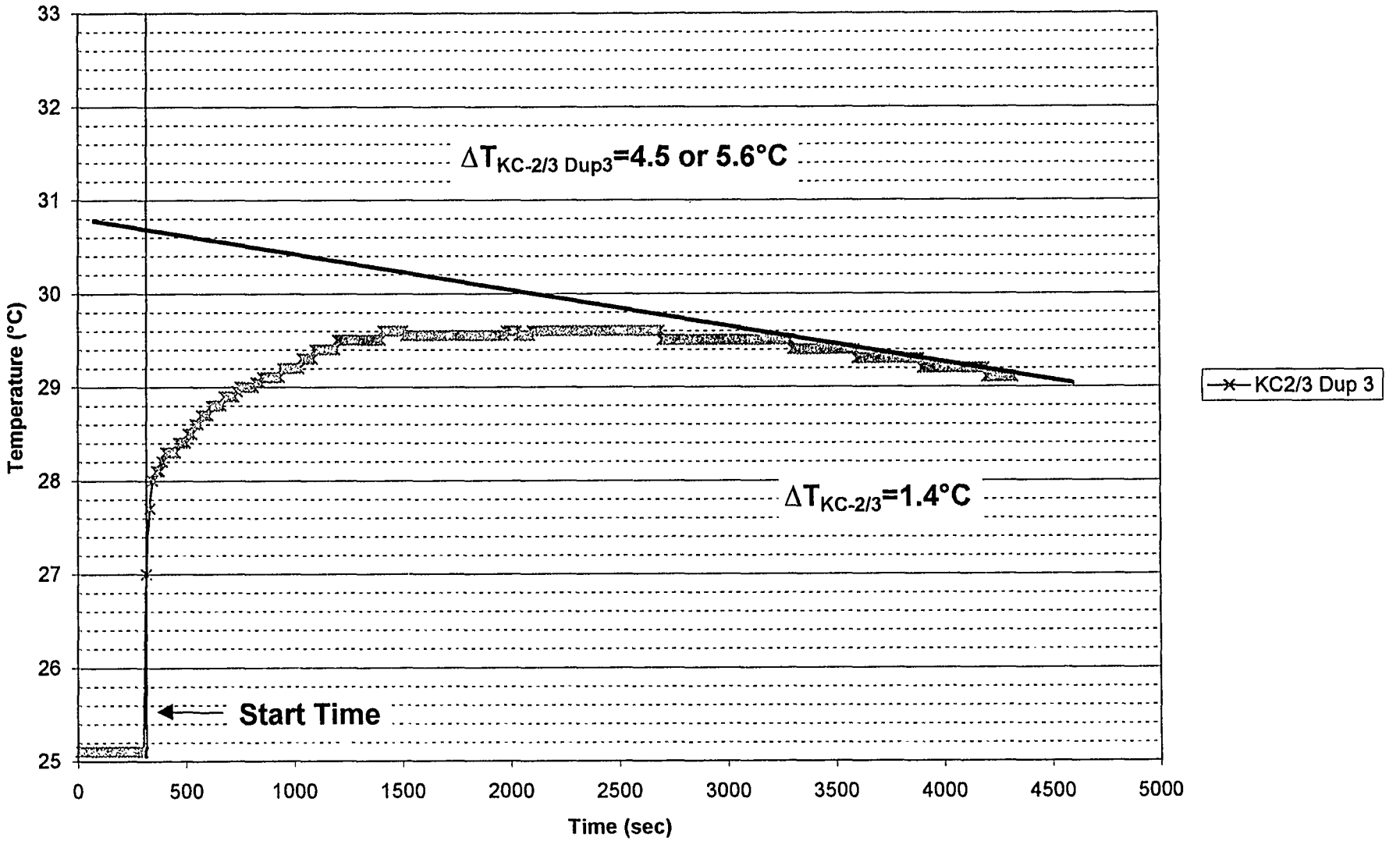

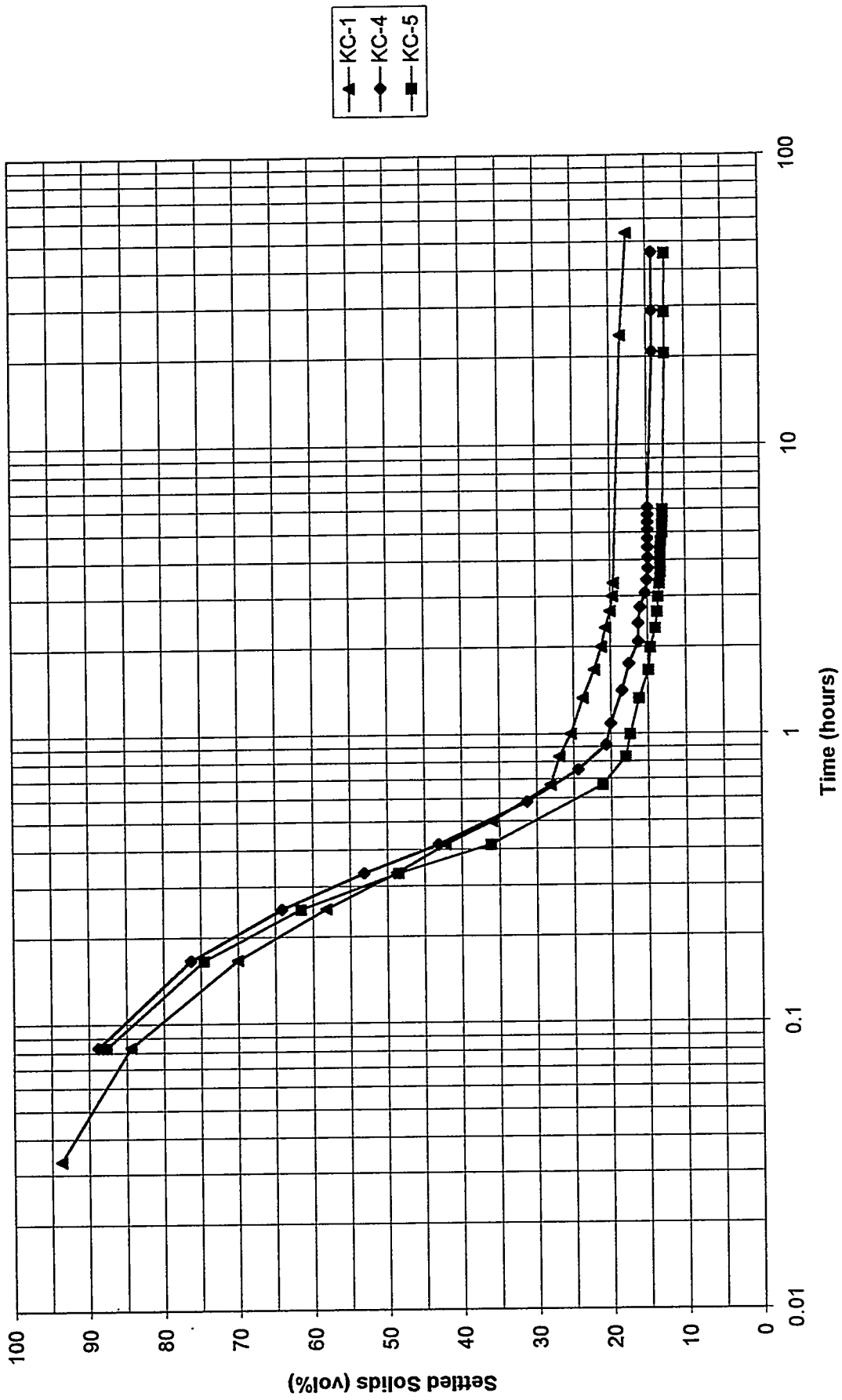

Figure 26. Volume Percent Settled Solids Versus Time for K East Basin Consolidated Samples

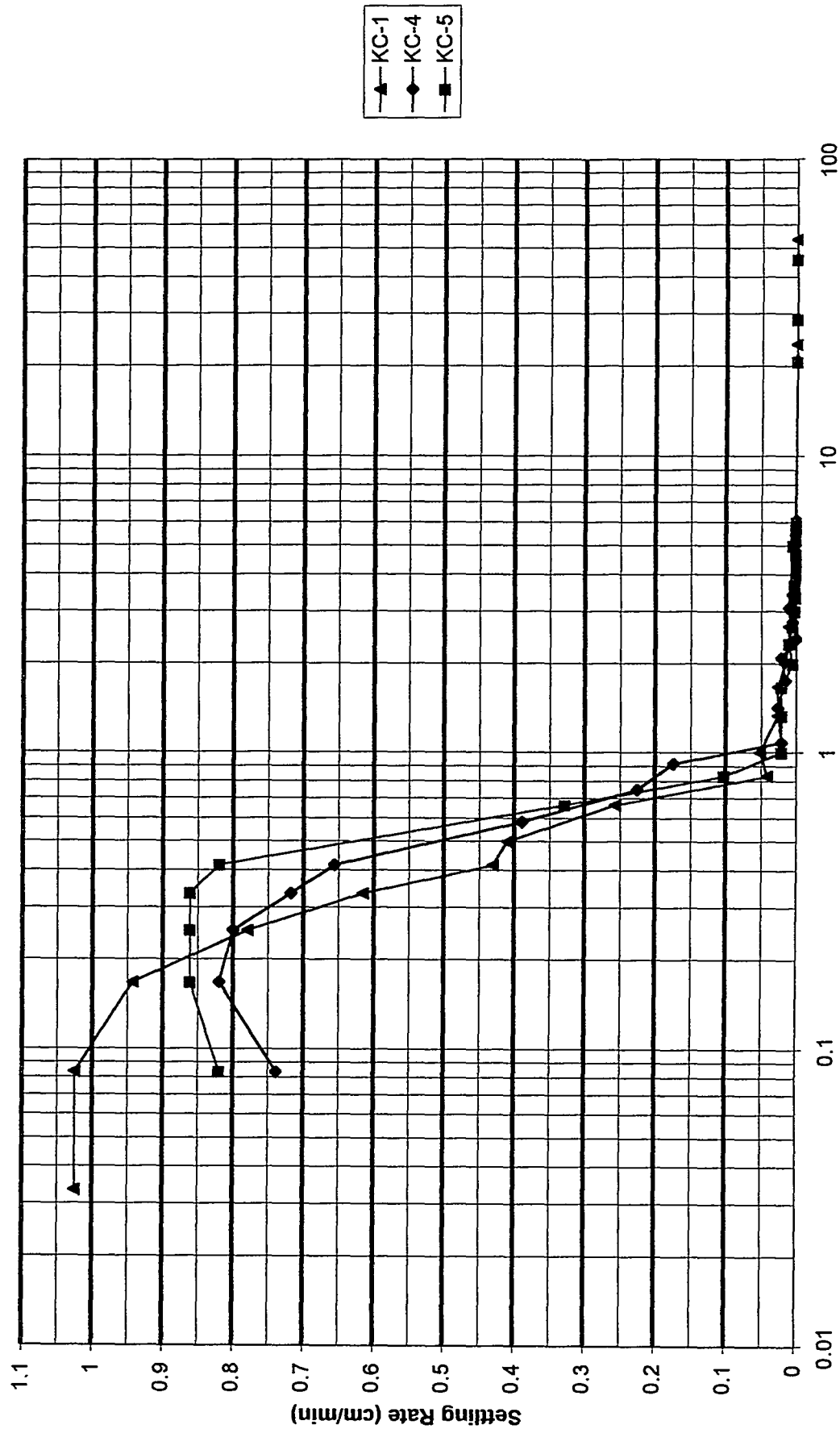

Figure 27. Settling Velocity for K East Basin Consolidated Sludge

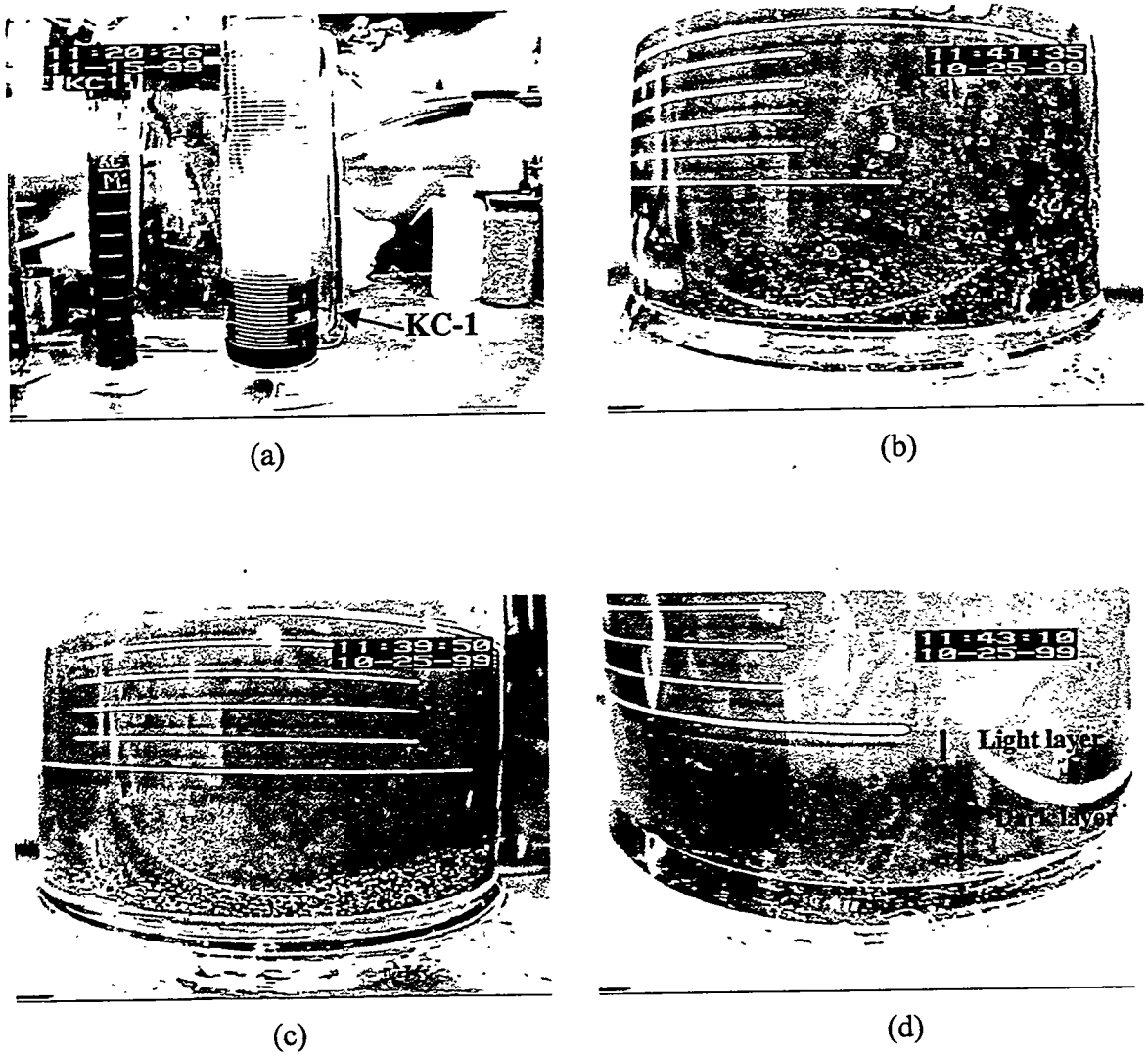

(a) (b)

(c) (d)

Figure 28. Samples from Settling Studies.
(a) KC-1 showed no layering following settling,
(b) a coarse layer settled on the bottom of KC-4,
(c) a similar coarse layer settled on the bottom of KC-5, and
(d) a light-colored layer is visible on top of a layer of darker-colored material from KC-2/3 M250. The supernatant in KC-2/3 M250 did not clear after approximately 2 weeks.

4.0 References

Baker, R. B., A. L. Pitner, T. L. Welsh, B. J. Makenas, and K. L. Pearce. 1999. *Sampling and Analysis Plan for Consolidated Sludge Samples from the Canisters and Floor of the 105-K East Basin.* HNF-4016, Rev. 0. Duke Engineering & Services Hanford, Inc., Richland, Washington.

Blaine, H. T. 1960. *Dissolution of Power Reactor Fuel Cores.* HW-66320, Hanford Atomic Products Operation, Richland, Washington.

Bredt, P. R., J. M. Tingey, and A. J. Schmidt. 1999. "Compilation and Integration of K Basin Sludge Particle Size Analysis Data." PNNL-13376 Pacific Northwest National Laboratory, Richland, Washington.

Gauglitz, P. A., S. D. Rassat, P. R. Bredt, J. H. Konynenbelt, S. M. Tingey, and D. P. Mendoza. 1996. *Mechanism of Gas Bubble Retention and Release: Results for Hanford Waste Tanks 241-S-102 and 241-SY-103 and Single-Shell Tank Simulants.* PNNL-11298, Pacific Northwest National Laboratory, Richland Washington.

Hecht, S. L. 1999. *System Design Description for the Consolidated Sludge Sampling System for K Basins Floor and Fuel Canisters.* HNF-3971, Rev. 0. Duke Engineering & Services Hanford, Richland, Washington.

Herrmann B. 1984. *Auflösung unbestrahlter UO_2-Pellets in Salpetersäure.* KfK 3673, Kernforschungszentrum Karlsruhe, Karlsrune, Germany.

Linde, D. R. 1993. *Handbook of Chemistry and Physics,* 49th ed. CRC Press, Ann Arbor, Michigan 1993.

Makenas, B. J., T. L. Welsh, P. R. Bredt, G. R. Golcar, A. J. Schmidt, K. L. Silvers, J. M. Tingey, A. H. Zacher, and R. B. Baker. 1999. *Analysis of Internal Sludge and Cladding Coatings from N-Reactor Fuel Stored in Hanford K Basins.* HNF-3589, Rev. 0, Fluor Daniel Hanford, Richland, Washington.

Makenas, B. J., T. L. Welsh, R. B. Baker, G. R. Golcar, P. R. Bredt, A. J. Schmidt, and J. M. Tingey. 1998. *Analysis of Sludge from Hanford K West Basin Canisters.* HNF-1728, Fluor Daniel Hanford, Richland, Washington.

Makenas, B. J., T. L. Welsh, R. B. Baker, E. W. Hoppe, A. J. Schmidt, J. Abrefah, J. M. Tingey, P. R. Bredt, and G. R. Golcar. 1997. "Analysis of Sludge from Hanford K East Basin Canisters." HNF-SP-1201, DE&S Hanford, Inc., Richland, Washington.

Makenas, B. J., T. L. Welsh, R. B. Baker, D. R. Hansen, and G. R. Golcar. 1996. "Analysis of Sludge from Hanford K East Basin Floor and Weasel Pit." WHC-SP-1182, Westinghouse Hanford Company, Richland, Washington.

Pearce, K. L., S. C. Klimper, and T. A. Flament. 1998. *105-K Basin Material Design Basis Feed Description for Spent Nuclear Fuel Project Facilities, Volume 2, Sludge.* HNF-SD-TI-009, Vol. 2, Rev. 2. Numatec Hanford Corporation, Richland, Washington.

Petersen, C. A., A. J. Schmidt, and R. B. Baker. 1999. *Revised Sampling Campaigns to Provide Sludge for Treatment Process Testing. HNF-4015.* Numatec Hanford Corporation, Richland, Washington.

Pitner, A. L. 1999. *K East Basin Sludge/Sampling 1999 Campaigns.* HNF-4746, Rev. 0. Numatec Hanford Corporation, Richland, Washington.

Swanson J. L., L. A. Bray, H. E. Kjarmo, J. L. Ryan, C. L. Matsuzaki, S. G. Pitman, and J. H. Haberman. 1985. *Laboratory Studies of Shear/Leach Processing of Zircaloy Clad Metallic Uranium Reactor Fuel.* PNL-5708, Pacific Northwest National Laboratory, Richland, Washington.

Tereschenko, L. T. et al. 1968. "Equilibrium Between Nitrogen Oxides and Nitric Acid Solutions." *Zhurnal Priladnoi Khimii* 41(3):487.

Wagman D. D., W. H. Evans, V. B. Parker, R. H. Schumm, I. Halow, S. M. Bailey, K. L. Churney, and R. L. Nuttall. 1982. "The NBS Tables of Chemical Thermodynamic Properties." *Journal of Physical and Chemical Reference Data* 11, Supplement Number 2.